

2009

A novel synthesis and characterization of fluorescein isothiocyanate labeled poly(styrenesulfonate sodium salt)

Xiaowei Tong

Louisiana State University and Agricultural and Mechanical College, xtong1@lsu.edu

Follow this and additional works at: https://digitalcommons.lsu.edu/gradschool_theses



Part of the [Chemistry Commons](#)

Recommended Citation

Tong, Xiaowei, "A novel synthesis and characterization of fluorescein isothiocyanate labeled poly(styrenesulfonate sodium salt)" (2009). *LSU Master's Theses*. 1238.

https://digitalcommons.lsu.edu/gradschool_theses/1238

This Thesis is brought to you for free and open access by the Graduate School at LSU Digital Commons. It has been accepted for inclusion in LSU Master's Theses by an authorized graduate school editor of LSU Digital Commons. For more information, please contact gradetd@lsu.edu.

**A NOVEL SYNTHESIS AND CHARACTERIZATION OF FLUORESCCEIN
ISOTHIOCYANATE LABELED POLY(STYRENESULFONATE SODIUM
SALT)**

A Thesis

Submitted to the Graduate Faculty of the
Louisiana State University and
Agricultural and Mechanical College
in partial fulfillment of the
requirements for the degree of
Master of Science

in

The Department of Chemistry

By
Xiaowei Tong
B.S., Zhejiang University, 2006
December 2009

ACKNOWLEDGMENTS

First of all, I would like to give my deepest and sincerest thanks to my research advisor, Dr. Paul S. Russo, for his advices, patience, and constant encouragements throughout this work. His extensive knowledge in polymer science and academic manner will benefit me in my future study and life. I sincere thank to Dr Sreelatha (Latha) Balamurugan for her inspiration and assistance that is essential for my success in this project. My thanks also go to Dr Rafael Cueto. Thank you for your training and assistance in the GPC measurement. Thank you to my colleagues and friends, Derek Dorman, Cornelia Rosu, Melissa Collins, Javoris Hollingsworthy, for their help in my research work. I would also like to give my thanks to Dr Dale Treleaven, Dr Dan Pu, and Andew Weber for providing training and analytical equipment.

Finally, I want give my great appreciate to my parents. Their encouragement and love throughout my ups and downs. Without you I wouldn't be here.

TABLE OF CONTENTS

ACKNOWLEDGMENTS	ii
ABSTRACT	v
CHAPTER1 INTRODUCTION: DYNAMICS OF POLYELECTROLYTES IN SOLUTIONS AND FLUORESCENCE PHOTOBLEACHING RECOVERY	1
1.1 Polyelectrolytes in Solutions	1
1.1.1 Polyelectrolytes	1
1.1.2 Polyelectrolytes in Solutions	2
1.2 Dynamics of Polyelectrolyte in Solution	4
1.2.1 Dynamic Light Scattering for Studying Dynamic Properties of Polyelectrolyte in Solution	5
1.2.2 Diffusion of Low Molecular Weight Salt	7
1.2.3 Diffusion of Polyelectrolyte in Solutions	8
1.2.4 Interpretation of Dynamics of Polyelectrolyte in Low-salt or Salt-free Solutions	11
1.3 Fluorescence Photobleaching Recovey	15
1.3.1 Introduction	15
1.3.2 Advantages of FPR	17
1.3.3 Instrument of FPR	18
1.3.4 Theory of FPR	19
1.3.5 Sample Labeling	21
1.4 Statement	23
CHAPTER2 SYNTHESIS AND CHARACTERIZATION OF FLUORESCEIN ISOTHIOCYANATE LABELED POLY(STYRENESULFONATE SODIUM SALT)	26
2.1 Introduction	26
2.2 Experimental	28
2.2.1 Materials	28
2.2.2 Synthesis of FITC-labeled 4-Aminostyrene	28
2.2.3 Synthesis of Poly(Styrenesulfonate Sodium Salt)	29
2.2.4 Synthesis of Poly(FITC-labeled Aminostyrene- <i>co</i> -styrenesulfonate Sodium Salt)	30
2.2.5 Purification of Poly(FITC-labeled Aminostyrene- <i>co</i> -styrenesulfonate Sodium Salt)	31
2.2.6 Characterization	31
2.3 Results and Discussion	33
2.3.1 FITC-labeled 4-Aminostyrene	33
2.3.2 Unlabeled NaPSS and FITC-labeled NaPSS	33

2.3.3 Fluorescence Properties of Poly(FITC Aminostyrene- <i>co</i> -styrenesulfonate Sodium Salt)	39
2.3.4 GPC Fractions of FITC-Labeled NaPSS	41
2.4 Conclusions	42
CHAPTER3 OPTICAL TRACER DIFFUSION STUDIES OF POLYELECTROLYTE SOLUTIONS	44
3.1 Introduction	44
3.2 Methods	46
3.3 Results and Discussion	48
3.3.1 Density of NaPSS Solution	48
3.3.2 Self-diffusion of GPC Fractions with FPR	49
3.4 Conclusions	51
REFERENCES	53
APPENDIX A: PERMISSIONS	57
APPENDIX B: LIST OF ABBREVIATIONS AND SYMBOLS	63
VITA	65

ABSTRACT

The diffusion of polyelectrolytes in low-salt or salt-free aqueous solutions is a controversial question. It has been intensively discussed since it was discovered in 1978. Most previous experimental data were obtained from dynamic light scattering (DLS), whose precision, however, was reduced by stringent sample preparation and weak scattering of polyelectrolyte in low-salt solution. For the most commonly studied polyelectrolyte, poly(styrenesulfonate sodium salt) (NaPSS), the harsh polymerization condition and the manufacturing procedure lead to hydrophobic defects and aggregations, which also block a correct insight about the diffusion of polyelectrolyte. In contrast to DLS, fluorescence photobleaching recovery (FPR) directly looks on the optical trace of the self-diffusion of labeled molecule and is relatively insensitive to the thermodynamic interactions among the polymer. In this work, an efficient synthesis of fluorescein isothiocyanate (FITC) labeled poly(styrenesulfonate sodium salt) (NaPSS) under mild conditions is presented. This fluorescent polyelectrolyte, with 100% degree of sulfonation and no hydrophobic defects, was directly synthesized from monomer. The product was characterized by mass spectrometry, GPC/MALLS, ^1H NMR, and fluorimetry. Twelve fractions with various molecular weights were obtained by injecting the sample solution into an analytical-scale GPC. The self-diffusion of some fractions was measured with FPR. The dependence of the diffusion coefficient on molecular weight is in agreement with the power-law. The partial specific volume of NaPSS in aqueous solution and salt solution were also determined by examining the densities of these solutions.

CHAPTER 1 INTRODUCTION: DYNAMICS OF POLYELECTROLYTES IN SOLUTIONS AND FLUORESCENCE PHOTOBLEACHING RECOVERY

1.1 POLYELECTROLYTES IN SOLUTION

1.1.1 POLYELECTROLYTES

Polyelectrolytes are polymer chains containing a variable amount of ionizable monomers. These groups can dissociate in aqueous solutions and make the polymers charged by leaving ions of one sign bound to the chain and dissociating counterions in solution. In contrast to most neutral organic-soluble polymers, polyelectrolytes are significant for being soluble in water.

Polyelectrolytes are everywhere around us and in us. Most biopolymers, including DNA and proteins, are polyelectrolytes, and many water-soluble polymers of industrial interest are charged. The polyelectrolytes combine both properties of electrolytes and polymers. Their solutions are electrically conductive like electrolytes and often viscous like polymers. Some polyelectrolytes can dissociate completely in solutions for most reasonable pH values. They are said to be strong electrolytes, e.g., with SO_3H units derived from a strong acid (Figure 1.1 (b)), all monomer units are dissociated, and the charges are said to be quenched. Others are said to be weak polyelectrolytes. Their charged monomer units are derived from a weak acid or base, e.g., monomers with COOH groups (Figure 1.1 (b)). In solution, not all groups are dissociated, and the degree of dissociation depends on the pH of the solution; each chain can be viewed as a random copolymer of monomers with COO^- and COOH groups that fluctuate; the distribution of charges are controlled by the pH, concentration of counterions, and polyions. The physical properties of polyelectrolyte

solutions are also affected by the degree of dissociation.

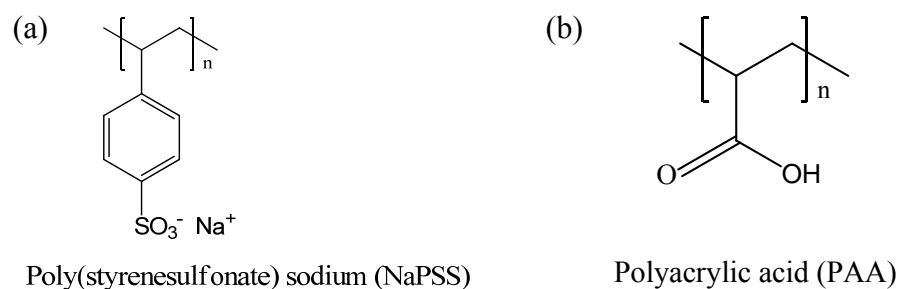


Figure 1.1 Examples of polyelectrolyte for (a) strong polyelectrolyte, (b) weak polyelectrolyte

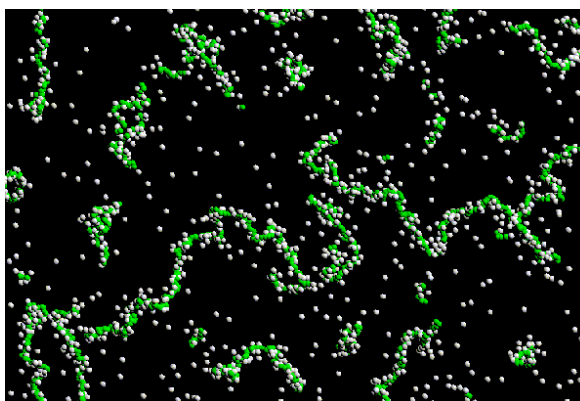


Figure 1.2 A snapshot of a configuration of polyelectrolytes and their dissociated counterions from a molecular dynamics simulation.² Reprint with the permission of Dr. Craig Pryor and Dr. James Donley

1.1.2 POLYELECTROLYTES IN SOLUTIONS

The solution properties of polyelectrolytes have been studied for more than 50 years. In the case of flexible polyelectrolyte solutions, the strength of electrostatic interaction is mainly influenced by the presence of a low-molecular-weight salt, which screens charges. In the region of high salt concentration, the polyelectrolyte chains behave similarly to flexible neutral macromolecules. This behavior has been understood well in terms of the scaling theory.³

A much more complicated situation arises if we want to understand the behavior

of a polyelectrolyte solution in the region of low salt or salt-free concentrations. In some cases a qualitative understanding is available but a quantitative interpretation is still lacking. For the others, even the origin of the phenomena observed remains partially obscure. This indicates the present treatments of polyelectrolyte behavior are incomplete and that some fundamental new views are needed to obtain a full understanding. Although a considerable of polyelectrolyte investigations have been done through different experimental methods, including static and dynamic light scattering,⁴⁻¹⁰ small-angle x-ray scattering (SAXS),¹¹⁻¹⁴ small-angle neutron scattering (SANS),¹⁵⁻¹⁸ viscosity,¹⁹⁻²¹ and NMR, they very often lead to controversial conclusions. This situation is due to the fact that experiments on polyelectrolytes always turned to be extremely difficult. A unique insight on the structure and the dynamical behavior of polyelectrolyte solutions are intensively prohibited by several aspects:

1. In contrast to the properties of the well understood “ordinary phase” (when the salt is in excess and the single polyelectrolyte chain is observable), the polyelectrolyte will form large and unidentified objects with co-ions when it is in the low-salt or salt-free solutions.
2. For the flexible polyelectrolytes, their shapes change with the ionic strength. Such a conformational change imposes another challenge on the understanding of flexible polyelectrolytes. It is still controversial what structure of the flexible polyelectrolyte forms at low ionic strength.
3. For all value of c_p/c_s (c_p is the concentration of polyelectrolyte, c_s is the

concentration of added salt), the properties of the polyions are additionally controlled by absolute value of added salt.

So far, polyelectrolytes have found a widening field of applications based on their specific properties. For example, they have been employed to either stabilize colloidal suspensions or to initiate precipitation. They are used to impart a surface charge to neutral particles, enabling them to be dispersed in aqueous solutions. In our daily life, they appear as conditioners, flocculants, drag reducers, and even some ingredients of food. They also make contributions to the investigation of biochemistry and pharmacy. There have been numerous of papers regarding the using of polyelectrolytes for implant coatings, for controlled drug delivery, for self-assembled films in polymeric sensors, for artificial muscles and other applications.²² The polyelectrolyte models have been used to analyze the structure and behavior of biomacromolecules, such as DNA, RNA and proteins.^{23, 24} Therefore, the current confusing situation of polyelectrolyte solution is far from satisfactory, and more thorough investigations are in strong demand.

1.2 DYNAMICS OF POLYELECTROLYTE IN SOLUTION

Among those complex and controversial properties of polyelectrolytes in solution, the presence of multipolyion domains in polyelectrolyte solutions is intensively discussed since they were first discovered by Schurr: a very slow diffusion mode of poly-L-lysine in low salt range was reported.²⁵⁻²⁷ Figure 1.3 shows this phenomenon: at a certain ratio of c_p/c_s , there is an accompanying drastic decrease in the diffusion coefficient and an increase in scattering intensity observed by dynamic light scattering.

The value of this ratio is only known approximately, varying from $1 \leq c_p/c_s \leq 5$ for monovalent counterions.

Later, more investigations indicated^{5-7, 10, 28-30} that such a “slow mode” can be found for essentially all studied polyelectrolytes, and this behavior is universally govern by the ratio of c_p/c_s . Although this phenomenon was attributed to the formation of an “extraordinary phase”,^{31,32} it does not means that this behavior is due to a phase transition. It is not appropriate to simply adopt this term of “extraordinary phase”.

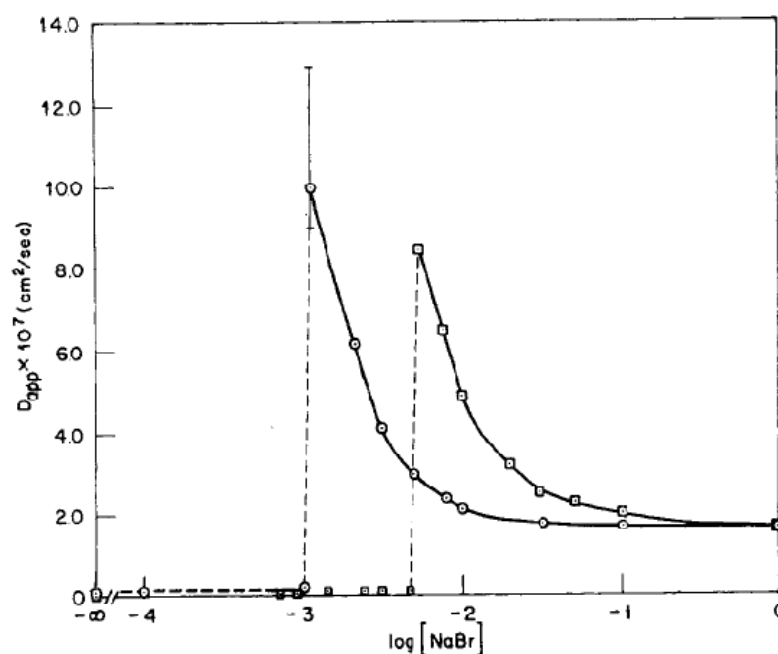


Figure 1.3 Apparent diffusion coefficient D_{app} vs $\log[\text{NaBr}]$ for poly(L-lysine)•HBar (DP=955) at $t=22-23^\circ\text{C}$ at pH 7.8. Circle denote 1.0 mg/mL and squares denote 3.0 mg/mL (Lys)_n.²⁵ Reprinted with permission of John Wiley & Sons, Inc.

1.2.1 DYNAMIC LIGHT SCATTERING FOR STUDYING DYNAMIC PROPERTIES OF POLYELECTROLYTE IN SOLUTIONS

Various experimental techniques have been used to study the dynamic properties of polyelectrolyte in solutions, including light scattering, small-angle neutron scattering (SANS), small-angle x-ray scattering (SAXS), electrophoretic light

scattering, viscosity, and NMR. Among them, Dynamic Light Scattering (DLS) is the most common method for examining the diffusion coefficient of polyelectrolytes in solution. Most published papers, mentioned in this study, are based on the experimental data of DLS.

In the DLS experiment, the intensity auto-correlation function is defined as

$$G^{(2)}(t) = \langle I(0)I(t) \rangle = \lim_{T \rightarrow \infty} \frac{1}{2T} \int_{-T}^T I(t')I(t'+t)dt' \quad \text{Eq. 1. 1}$$

Where t is the delay time and $I(t)$ is the time-average scattering intensity.

The correlation function is converted into the normalized second-order correlation function using the relation:

$$G^{(2)}(t) = B(1 + f|g^{(1)}(t)|^2) \quad \text{Eq. 1. 2}$$

Where B is the baseline, and f is an instrumental parameter ($0 < f < 1$).

In many cases, the electric field autocorrelation function, $g^{(1)}(t)$, is a single exponential:

$$g^{(1)}(t) = e^{-\Gamma t} \quad \text{Eq. 1. 3}$$

Where Γ is the decay rate (the inverse of the correlation time). The translational diffusion can be calculated according to:

$$\Gamma = \tau^{-1} = q^2 D_m \quad \text{Eq. 1. 4}$$

Where D_m is the mutual diffusion coefficient, q is the scattering vector, $q = \frac{4\pi n}{\lambda_0} \sin \theta$, with n as the refractive index of the sample, λ_0 as the incident laser wavelength in vacuo, and θ as scattering angle.

In a polyelectrolyte solution, several processes with different relaxation rates, Γ , are expected to contribute to $g^{(1)}(t)$. The distribution function, $A(\Gamma)$, of the

amplitudes of Γ and $g^{(1)}(t)$ are related by Eq. 1.5

$$g^{(1)}(t) = \int_0^{\infty} A(\Gamma) \exp(-\Gamma t) d\Gamma \quad \text{Eq. 1.5}$$

For example, when $g^{(1)}(t)$ contains two distinguishable relaxation modes, it can be analyzed using a combination of two exponential functions

$$g^{(1)}(t) = A_f \exp(-\Gamma_f t) + A_s \exp(-\Gamma_s t) \quad \text{Eq. 1.6}$$

Where A_f and A_s are amplitudes.

Solving Eq. 1.6 is known as a Laplace inversion. The conversion can be carried out by program CONTIN.^{33,34}

1.2.2 DIFFUSION OF LOW MOLECULAR WEIGHT SALT

Because the low molecular weight salt ions in polyelectrolyte solutions are counterions and co-ions and have an effect on the electrostatic field, it is appropriate to mention their dynamic properties here. Compared to macromolecules, these small ions have a very fast diffusion process and a low scattering contribution observed by light scattering experiments. Although this fast diffusion rate is still relatively well within the capability of current dynamic light scattering instrumentation, the extremely weak scattering signal due to the small size of such ions poses a problem. Therefore, the measurement of the small ion diffusions by light scattering is difficult. One of the more interesting papers to explore counterions specifically was reported by Marian Sedlak *et al.*⁴ He successfully measured the diffusion of small ions in a pure solution and in a “mixture with polyions”. They reported that the corresponding diffusion coefficient of small ion can be expressed as

$$D_c = \frac{\Gamma_2(q)}{q^2} = \frac{(1 + \left|\frac{Z_b}{Z_a}\right|)D_a D_b}{D_a + |Z_b/Z_a|D_b} \quad \text{Eq. 1. 7}$$

Where $\Gamma_2(q)$ is the inverse relaxation time, q is the scattering vector, $q = \frac{4\pi n}{\lambda_0} \sin \theta$, D_a and D_b are the values of uncoupled diffusion coefficient of particular ions, and Z_a and Z_b are the charges. This predicted value by this equation agrees with the value of experimentally obtained diffusion coefficient.

1.2.3 DIFFUSION OF POLYELECTROLYTE IN SOLUTIONS

Polyelectrolyte solutions in practice have a wide of molecular weight distribution and should be principally considered as mixtures. Besides, polyions are not always distributed homogeneously in solutions and mixtures, but instead may form larger structures referred to as domains or clusters. These structures also contribute to the overall scattering intensity and can be therefore considered as an additional component of the system.

The diffusion of polyions in polyelectrolyte solutions is strongly influenced by three factors: 1) the effective charge of the polyion; 2) the concentration of added salt; and 3) the polyion concentration

For weak polyelectrolytes, a stronger dissociation is reached by adding counterions, which interact with dissociated polymer chain to effectively reduce high charge. The ratio of the molar concentration of added counterions to the monomer concentration of the polyions is defined as α . The diffusion coefficient of polyions increases upon increasing α and levels off at higher values of α . According to the Oosawa-Manning³⁵⁻³⁷ theory, the onset of counterion condensation corresponds to the situation where the mean intercharge spacing along the chain, A_c , equals the Bjerrum

length l_B , which defined as $l_B = e^2 / \epsilon k_B T$ (e is the electron charge, ϵ is the dielectric permittivity, k_B is Boltzmann's constant, and T is temperature).

For strong polyelectrolytes, the diffusion coefficient depends on the concentration of added salt. Generally, the mutual diffusion coefficient increases with the decrease of the added salt concentration, c_s . At high c_s , the diffusion coefficient of polyion is independent of the salt concentration, and the values resemble those of equivalent neutral polymers. The diffusion coefficient decreases with increasing molecular weight at high c_s . This is also similar to neutral polymers where the diffusion coefficient is inversely dependent on the friction factor, i.e., $D \propto f^{-1} \propto M^{-\beta}$, where f is the friction factor and β is the factor related with the structure of polymer in solution. On the contrary, the diffusion coefficient at low c_s is independent of molecular weight. The polyelectrolytes diffuse extremely slowly when the concentration of added salt is very low, which is termed as the extraordinary phase.

After the discovery of the “ordinary-extraordinary” transition, Schmitz, K. S.³⁸ *et al* reported that there were actually a fast mode and a slow mode diffusion simultaneously existing in DLS measurements of salt-free or low-salt dilute polyelectrolyte solutions in comparison with the translational diffusive relaxation mode of individual neutral chains with similar lengths.³⁹ Later, this splitting of relaxation mode were verified by both synthetic and biological polyelectrolytes in low-salt or salt-free solutions.

So far, various experimental data indicate that the fast-mode diffusion coefficient, D_f , is independent of molecular weight, while the slow-mode diffusion coefficient, D_s ,

decreases with the increase of molecular weight. Figure 1.5 and Figure 1.6 shows the dependence of D_f and D_s on the molecular weight in logarithmic coordinates, respectively. The sample used is NaPPS in $c = 45.6$ g/L with the scattering angle $\theta = 90^\circ$

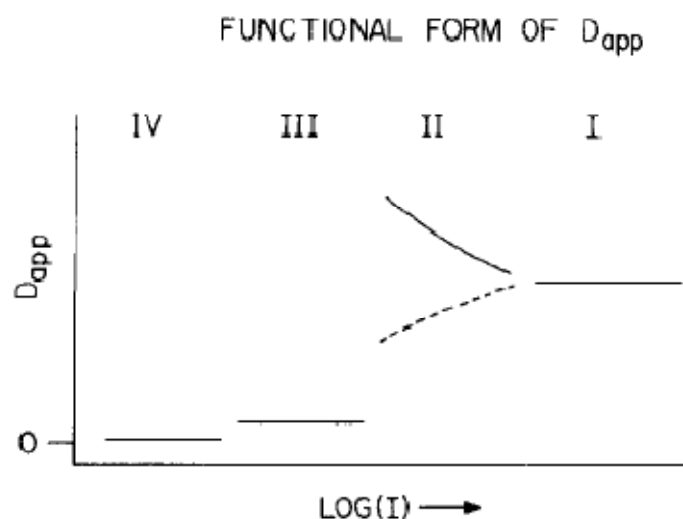


Figure 1. 4 Schematic partitioning of D_{app} as a function of ionic strength. Reprinted with permission from [39]. Copyright 1983, American Institute of Physics.

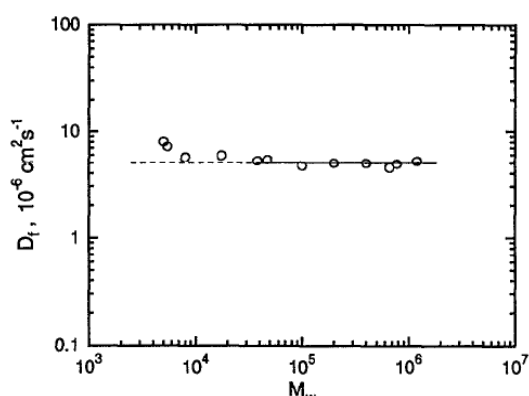


Figure 1. 5 Dependence of fast-mode diffusion coefficient D_f on molecular weight. Reprinted with permission from [5]. Copyright 1992, American Institute of Physics

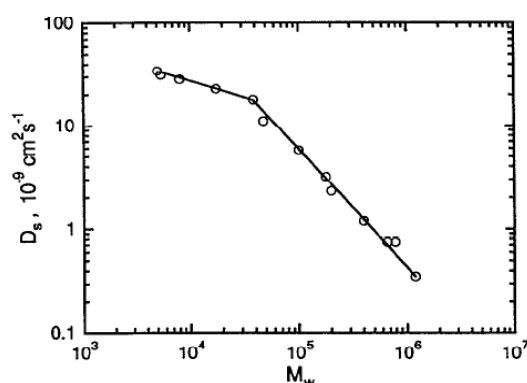


Figure 1. 6 Dependence of slow-mode diffusion coefficient D_s on molecular weight. Reprinted with permission from [5]. Copyright 1992, American Institute of Physics.

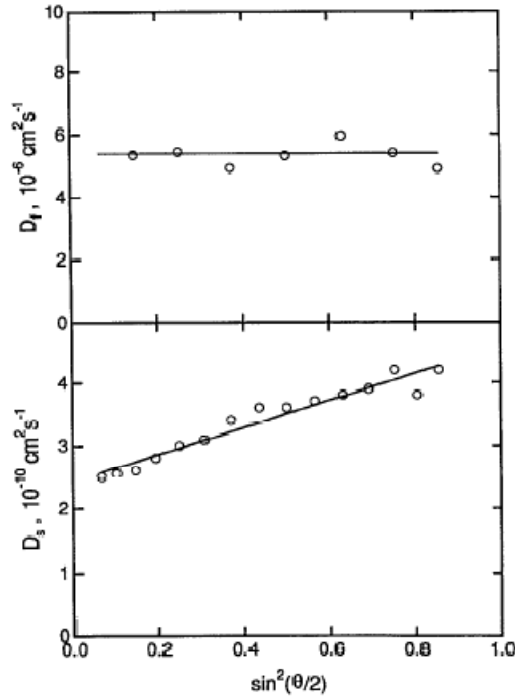


Figure 1. 5 Dependencies of diffusion coefficients D_f and D_s on scattering angle θ : $M_w = 1\,200\,000$, $c = 45.6$ g/L. Reprinted with permission from [5]. Copyright 1992, American Institute of Physics

The light scattering measurements show that D_s increases with scattering angle while D_f is nearly independent of scattering angle. Figure 1.7 shows the linear function of D_s vs $\sin^2\left(\frac{\theta}{2}\right)$ and the independence of D_f on the molecular weight.

1.2.4 INTERPRETATION OF DYNAMICS OF POLYELECTROLYTE IN LOW-SALT OR SALT-FREE SOLUTIONS

Several different theoretical models have been developed for interpretation of various experimental data taken in low-salt or salt-free solutions. Lifson and Katchalsky⁴⁰ assumed that charged macromolecular chains are rigid-like rods because of very strong, unscreened repulsive interactions between charges along the chain. It was suggested that there is a hexagonal structure with the parallel ordering which is due to the intermolecular interactions.

DeGennes⁴¹ *et al.* summarized the behavior of polyelectrolytes in solutions as a function of polymer concentration. They examined several concentration regions and distinguished the critical concentrations. At the lowest polymer concentration, the intermolecular interactions are reduced by the large separation between polymer chains. The polyions are fully stretched and behave like single molecules. When concentration moves to higher regime, the intermolecular interactions become larger and the polyions cannot freely orient any longer. They may form an ordered lattice. Further increasing the concentration gives rise to an overlap of chains and formation of a transient network. Under these conditions macromolecules become more flexible, and a characteristic correlation length, ζ , can be introduced to describe the system. In this model there is no direct contact between chains because of repulsive electrostatic interactions.

The isotropic model of de Gennes was later reconsidered by Odijk,³ who derived scaling relations based on the concept of an electrostatic persistence length. It takes into account the electrostatic contribution from the polyelectrolyte effect of increased stiffness of chains. The total persistence length L_t is then given as a sum of the electrostatic persistence length L_e and persistence length L_p which characterizes the chain stiffness in the absence of charges. The persistence length L_t decreases with the concentration as c^{-1} . A critical concentration c^* is introduced when $L_t \approx l$, where l is the contour length of the polyelectrolyte. Three different regimes are defined for $c > c^*$. For $c^* < c < c^{**}$ the tridimensional lattice is deformed but retains some anisotropy. This is the regime where $L_t \gg \zeta$. Above c^{**} (the concentration where the lattice melts),

the system is in an isotropic phase with $L_t \ll \zeta$, and the macromolecule may be viewed as an ideal chain of “blobs” with average dimension ζ . Each blob is treated as a wormlike chain with fully exerted excluded-volume effect. In the former regime, we have $\zeta \sim c^{-1/2}$ and $R \sim c^{-1/2}$, and in the latter we have $\zeta \sim c^{-3/8}$ and $R \sim c^{-5/16}$ or $\zeta \sim c^{-5/8}$ and $R \sim c^{-3/16}$ for the case when $L_t \approx L_e$ or $L_t \approx L_p$, respectively. Table 1.1 describes the details of these regimes.

Table 1.1 The phase diagram for aqueous polyelectrolyte solution without added salt.

Region	Conc. range	Qualitative remarks
A	$c_G^* \gg c$	Very dilute; negligible interaction between the polyions
B	$c^* > c > c_G^*$	Dilute/semidilute; polyions remain rigid and interact strongly
C = III	$c^{**} > c > c^*$	Drastic decrease in the viscosity due to large decrease in polyion dimension
D = I + III	$c_4 < c < c^{**}$	Fuoss law; chain behavior
E	$c > c_4$	Rouselike polymer behavior

Muthukumar^{42,43} calculated the excluded volume of polyelectrolyte in solution as a function of various ions concentrations. He proved that the bare excluded volume interaction and the electrostatically screened Coulomb interaction between any two segments are both screened by the presence of polyelectrolyte chains at nonzero concentration. This excluded volume screening leads to an attractive component in the effective potential interaction at intermediate distances between two segmental charges of the same sign.

Drifford⁴⁴ and Sedlak²⁸ proposed that the fast mode diffusion was a coupled diffusion of the charged species in solution: polyions and counterions. In this solution, the concentration fluctuation of counterions induces an electric force which attracts their surrounding polyions. The polyions were dragged by the much faster motion of counterions and result in the presence of fast mode diffusion.

The explanations proposed for the slow mode are interesting, but they have not been proved completely. Stigter⁴⁵ suggested that the slow mode might result from an isotropic-anisotropic transition in rodlike polyions due to repulsive polyion-polyion interactions. However, there is no optical evidence of orientation such as birefringence.

The concept of domains in solution has also been used to interpret results of dynamic light scattering experiments that show the occurrence of an extremely slow-diffusive mode for low-salt polyelectrolyte solutions.³⁹

Schmitz⁴⁶ *et al.* have proposed a temporal aggregate model. There are polyion clusters which coexist with the free polyions. To stabilize the clusters there is a balance of repulsive and attractive forces. The repulsive forces are random Brownian motions which favor disruption. Attractive forces are presumed to result from fluctuating dipole fields generated by the sharing of the small ions by several polyions. Although this model is quite attractive, there is no sufficient experimental data to confirm it.

There are also several theories^{47, 48} that treat polydispersity as the cause of the slow mode. That is, D_s represents exchange diffusion, i.e., diffusion of the local

degree of polydispersity. However, the slow mode is observed also when the polyion sample is nearly monodisperse, such as NaPSS. Alternatively, cluster formation might be viewed as a type of polydispersity.

1.3 FLUORESCENCE PHOTBLEACHING RECOVERY

1.3.1 INTRODUCTION

If a fluorescent sample is put under a fluorescence microscope, a phenomenon would be found that if one observes a fluorescent sample within a 40× objective for a long time, and then switches to a 10× objective, it may appear that a dark hole has been burned into the sample (Figure 1.8). This is variously known as photobleaching, fading, photofading, and photodecay. Photobleaching is mainly due to photochemical reactions induced by the light used for excitation. The absorption of light, prerequisite for fluorescence, entails the raising of molecules to the excited state. The excited state is virtually a different chemical species, usually much more reactive than in the corresponding ground-state molecule. A small but significant proportion of the excited molecules, instead of fluorescing, undergo a photochemical reaction with the production of a new molecule which may be non-fluorescent, or at least non-absorbent at the excitation wavelength.

The dark hole in the Figure 1.8 is burned by exposure to a bright light which is focused by the 40× objective. A recovery would be found after a period. This is caused by diffusive exchange between the bleached molecules and unbleached molecules in the rest of the sample.

Fluorescence Photobleaching Recovery (FPR) (also named as fluorescence

recovery after photobleaching (FRAP)) is a technique basing on the photobleaching. It measures the rates of simple transport processes such as diffusion or convective flow or rates of transport coupled with chemical reactions in open systems. The measurement can be described by three steps:

1. The fluorescence of a small, select region of the sample is measured using a illuminating light that is not strong enough to cause rapid degradation of the signal.
2. The fluorescent moieties in this defined region are irreversibly photobleached by exposure to a pulse of bright light.
3. The return of fluorescence to that same region, due to the exchange by diffusion of bleached molecules with unbleached molecules that originally lay outside the selected volume, is monitored.

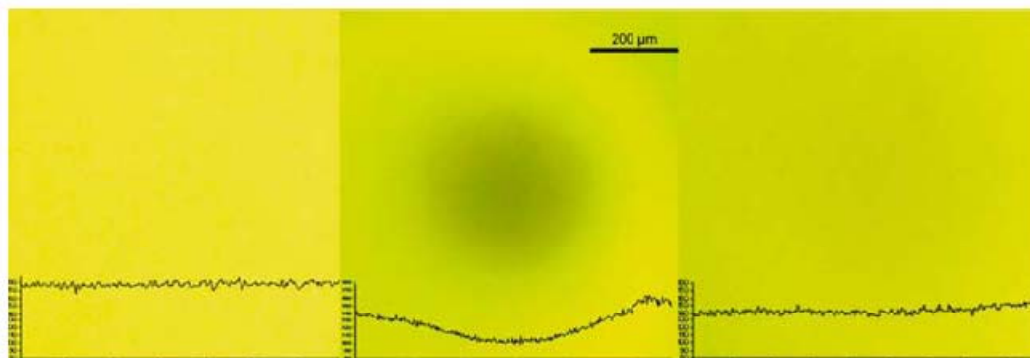


Figure 1. 6 FPR. Left: epifluorescence image acquired with 40× objective. Middle: after 10 min illumination, a spot has been bleached in the pattern, now taken with 10× objective. Right: recovery is almost complete after 30 min (still 10× objective). Traces show intensity across the middle of the image¹. Reprint with the permission of Springer.

Recovery of fluorescence is due to the diffusion or flow of the unbleached molecules in the surrounding region. Therefore, the analysis of recovery rate is related

to the self diffusion coefficient of the fluorescence molecules.

1.3.2 ADVANTAGES OF FPR

Currently, besides FPR, there are many other diffusion detective techniques commercially available, e.g., dynamic light scattering (DLS), analytical ultracentrifugaion (AUC), and diffusion ordered NMR spectroscopy (DOSY). Each of them has particular advantages: DLS with a modern correlator is able to study a wider range of diffusion coefficients in a single measurement than any competitor; DOSY excels at small, rapid diffusers that may not scatter enough light for DLS; and AUC can succeed at very low concentrations. All of these methods share the advantage over FPR that no fluorescent label need be attached or naturally present.¹

In return for the trouble of labeling the macromolecule, FPR offers unmatched selectivity: one exactly observes the diffusers that have been labeled. Compared with the mutual diffusion coefficient from DLS and AUC, the measured optical tracer less reflects the thermodynamic interaction. The optical tracer self diffusion coefficient is not quite the same as the self diffusion coefficient from DOSY, because the concentration gradient between bleached and unbleached molecules has an associated chemical potential gradient. It is expected to be very small, though, compared to chemical potential gradients arising from variations in the concentration of the macromolecules themselves, on which DLS and AUC rely. The optical tracer self diffusion coefficient from FPR can be collected over a much wider range of values than that DOSY can measure, and requires just microliters of sample.

1.3.3 INSTRUMENT OF FPR

The objective of FPR is to observe the transition of the fluorescence in a geometrically well-defined volume, which is defined by the illumination volume. FPR measurements are capable to study small systems. This advantage is obtained by using an epifluorescence microscope in conjunction with a laser as the illuminating light source. In this section, an equipment associated with a modulated-photobleaching is described because it enables shallow bleaches allowing each diffuser produces a single exponential decay. Figure 1.9 shows a simplified FPR instrument in our lab. It consists of an ion laser, an epifluorescence microscope, focusing, intensity modulation optics, a photomultiplier tube with photon counting electronics, accessory electronics for controlling shutters and protecting the photomultiplier tube, and computer interfacing for controlling the experiment and collecting the data.

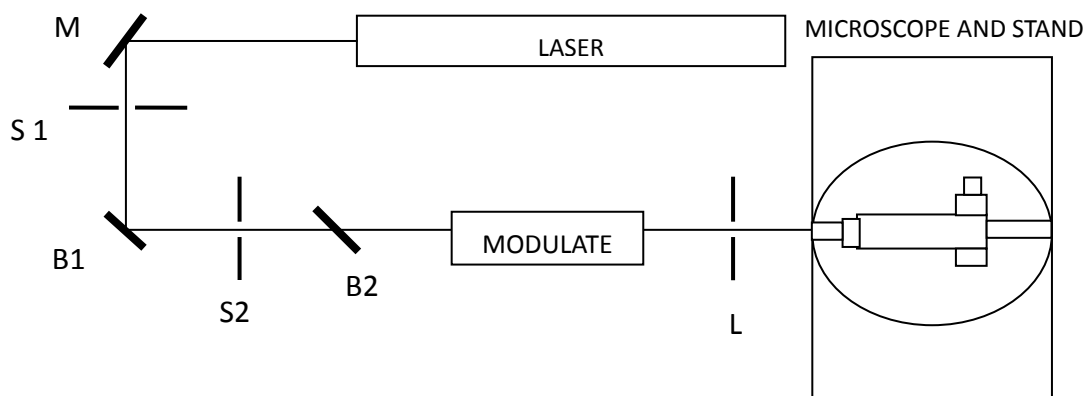


Figure 1. 7 Schematic representation of an FPR system. The laser beam is reflected by a mirror (M1) onto a beam splitter (B1) to maximize the reflection at the back surface. The weaker beam (the monitor beam) is passed unimpeded to the second beam splitter (B2) where it is recombined with the stronger beam (the bleach beam) after two internal reflections. The bleach beam is blocked (except during the bleach) by a shutter (S2). The beam is aligned with the optical axis of the microscope by a pair of mirrors (M2+M3) in a beam steerer. The single lens L provides the appropriate focusing prior to entry into the epifluorescence condenser of the microscope. The first shutter (S1) permits blocking of the entire beam between experiments.

1.3.4 THEORY OF FPR

In FPR experiments, the principal task is to measure the fluorescence transport from an open region of solution as a function of time. This is interpreted in terms of the concentrations or numbers of fluorescent labeled molecules in the observation region. The fluorescence intensity is expressed in terms of F . As showed in Figure 1.10, the F_0 and $F(\infty)$ is the pre-bleach intensity and the immediate post-bleach intensity, respectively. $F(\infty)$ is not always same as F_0 .

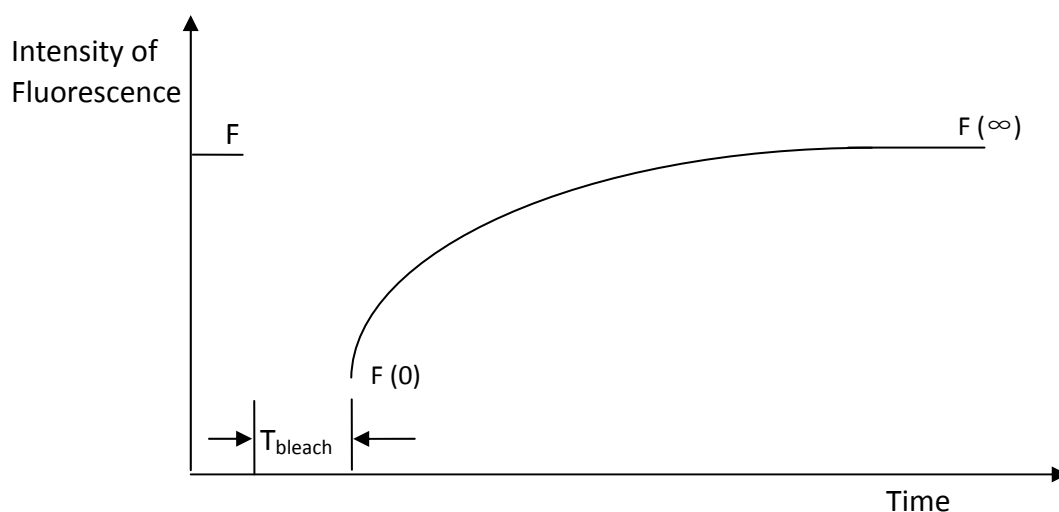


Figure 1. 8 Timing diagram for FPR experiment, with definition of terms

If $F(t)$ represents the fluorescent intensity at time t following a bleaching whose bleaching depth is characterized by parameter k , the value of k can be calculated as:

$$\frac{F(0)}{F^0} = k^{-1}(1 - e^{-k}) \quad \text{Eq. 1. 8}$$

The percentage of dye groups bleached can be calculated as

$$P = \frac{F^0 - F(0)}{F^0} \times 100\% \quad \text{Eq. 1. 9}$$

There are various bleaching patterns have been reported. A schematical summary

is showed as Figure 1.11

Currently, most FPR measurement is practiced by placing a mask on the rear image plane of the microscope and creating a pattern on the sample during the photobleaching step. Striped patterns are convenient because of the easy availability of Ronchi rulings, an optical element in which black stripes are etched into glass at a regular distance. If L represents the pattern size in the sample, the spatial frequency of the pattern is defined as $K= 2\pi/L$

The fluorescent sample after bleaching appears to a square wave in fluorescent intensity as a function of distance, x , which as showed in Figure 1.10. The bright and dark regions are equal in width. The diffusion of fluorescence in the pattern can be described in the Fourier series function:

$$F(x, t = 0) = F^0 - \frac{C}{2} + \frac{C}{2} \left[\frac{4}{\pi} \left(\sin(Kx) + \frac{1}{3} \sin(3Kx) + \frac{1}{5} \sin(5Kx) + \frac{1}{7} \sin(7Kx) + \dots \right) \right] \quad \text{Eq.1. 10}$$

The variable C represents the initial contrast:

$$C = |F^0 - F_{\min}(t = 0)| \quad \text{Eq.1. 11}$$

Where F_{\min} is the minimum intensity along the square wave pattern. Eq.1. 10 neglects edge effects at the boundary of the striped pattern and the circular or Gaussian illumination profile. The relaxation of the square wave pattern amounts to multiple simultaneous instances of diffusion in a sine wave boundary condition. This problem can be integrated by Fourier transform: the fundamental decays as $\exp[-DK^2t]$. Therefore, most exponential items in Eq 1.10 are ignorable, and only a few terms are needed to represent the fluorescence recovery integrated over all x . The signal obeys to:

$$F(t) = F^0 - \frac{C}{2} - \frac{C}{2} \frac{e^{-DK^2t} + \frac{1}{3}e^{-9DK^2t} + \dots}{1 + \frac{1}{3} + \dots} \quad \text{Eq. 1.12}$$

This equation can be handled by a nonlinear fit package. If C is estimated, it also can be linearized except for the first few data points at early times. Usually, a constant baseline term B or a function $B(t)$ would be added to address the recovery incompleteness or a nominally slanted background caused by the spot recovery process.

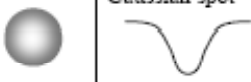

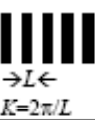



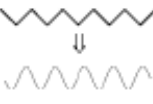


Category	Pattern	Detected	Ref.	Comments
Spot		Profile itself	2,3	Most common.
Spot		Profile itself	44	
Stripe		Ronchi ruling 	Sum of Fourier components of square wave	5,6 Provides periodic boundary condition.
Modulated		Ronchi ruling 	Usually triangle wave filtered to sine 	47 Enables shallow bleaches, each diffuser produces a single exponential decay.
		Crossed beams 	Depends on modulation scheme	16,54,55 Enables much shorter spatial distances.
Video	Varies	Mask	FFT	112 Fewer moving parts, multiple K values simultaneously measured.

Figure 1.11 Various types of photobleaching patterns.¹ Reprint with the permission of Springer

1.3.5 SAMPLE LABELING

Compared with other diffusion detectors, FPR experiments take advantage of the selectivity and sensitivity of fluorescence spectroscopy. The price for these

advantages is the frequent necessity to use fluorescien or its derivate as probe. In studies of diffusion or aggregation, the probe is likely to be small. In studies of chemical kinetics, it is probable that the rates of reactions and the equilibrium constants may be affected by the probe. In such cases the choice of probe and/or the site of labeling may greatly affect the results and alternatives should be explored.

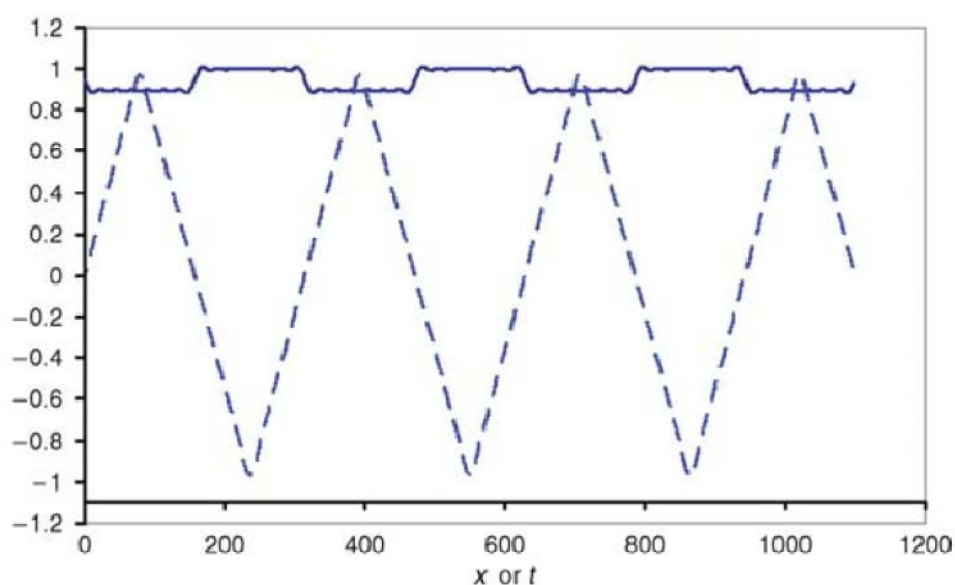


Figure 1. 12. A modulation detector functions to convert a shallow, typically 5-10%, spatial modulation in fluorescent intensity (solid line, in this case almost a square wave) into a large, time-dependent voltage (dashed line, in this case almost a triangle wave).¹ Reprint with the permission of Springer.

There are some concerns about the species of fluorescent probe. First, since the fluorescence microscope generally employs ion-lasers for illumination, the fluorophore must absorb in the region 450-530 nm or 514.5-660 nm depending on the laser type. Second, the probe must be photostable., so that little photolysis occurs during the observation of the recovery of fluctuations. Yet for FPR experiment, it is necessary that the probe can be irreversible photolysed so that the developed theories are applicable to the data analysis. Furthermore, it is desirable to maximize the

fluorescence quantum yield to enhance the sensitivity. A number of quite different fluorephores satisfy most of these criteria, and some of these are listed in the Table 1.2 along with their chemical structure shown in Figure 1.13.

There is no strict guideline about how many dye molecules to attach. Too many dyes can affect the structure of the macromolecule. It is proposal that photobleaching byproducts may cut neighboring chains and result in too-rapid diffusion for the damaged polymer. Since FPR exhibits excellent sensitivity, trace amount of labeling results in adequate signal. For uniform macromolecules, it is better to start by adding enough dye to label one in ten or one in a hundred macromolecule.

1.4 STATEMENT

In the study of this thesis, a fluorecein isothiocyanate(FITC) labeled poly(styrenesulfonate sodium salt) is polymerized through the ATRP. The synthesis is started from monomer, styrenesulfonate, and gives 100% sulfonate degree to the product. This synthesis also takes advantage of the living feature of ATRP which results in a narrow polydispersity. The attachment of FITC label was confirmed by mass spectroscopy, fluorescence spectroscopy, and fluorescent photobleaching recovery. The level of labeling was estimated with fluorimeter. This labeled NaPSS was then separated into 12 different fractions by rejecting the sample solution into an analysis scale GPC/MALLS. The self-diffusion of these fractions were investigated by means of FPR .

Table 1.2 Some commonly used fluorescent molecules

Fluorescent probe	$\lambda_{\text{ex}}^{\text{max}}$ (nm)	$\lambda_{\text{em}}^{\text{max}}$ (nm)	ϕ_f	Comments
Fluorescein (1)	490	520	0.15-0.3	ϕ_f depends on degree of labeling because of self-quenching. Emission is pH sensitive. Photostable
Tetramethylrhodamine (2)	550	580	0.1	Fairly hydrophobic and chemistry of labeling is harder in aqueous media. Extensive dialysis needed. Photostable
Eosine (3)	522	560 (690)	Very low phosphorescence	Good probe for rotational diffusion. Low fluorescence yield is less good for FPR measurements
Lissamine rhodamine (4)	540	570	Low	Easier to label with than (2) but lower ϕ_f .
Nitrobenzoxadiazole (NBD-Cl)(5)	340(-Cl) 430(-SR) 470(-NHR) 480(-NR ₂)	--- 520 530 530	0 --- 0.05 0.05	Good probe to react with SH or amino groups. NBD-Cl is not fluorescent. Emission wavelength and yield are very solvent dependent. Photostable
NBD-methyl amino-hexanoic acid-NHS (6)	480	535	0.05	Developed to react with hindered amines

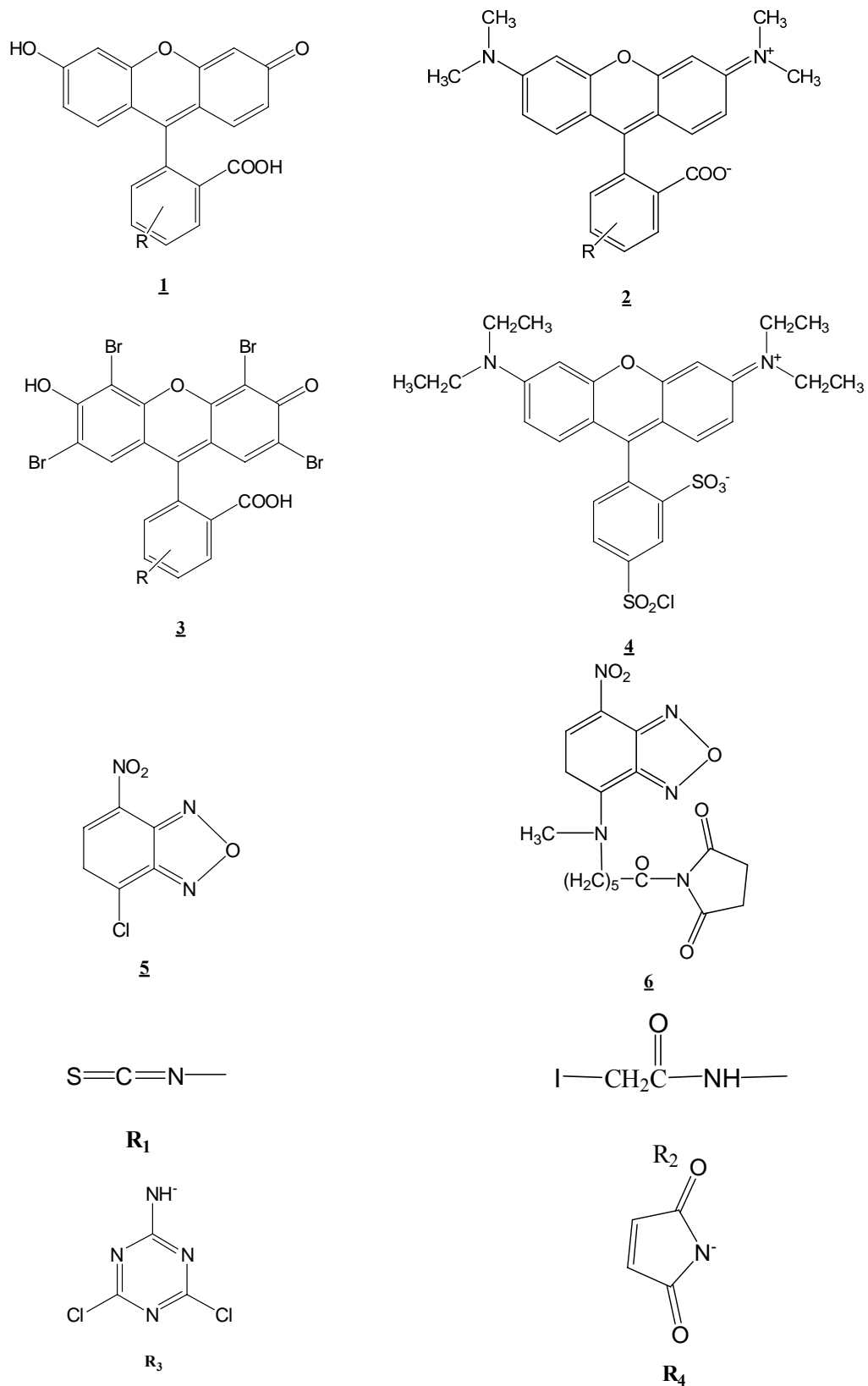


Figure 1.13 Chemical structures of some commonly used fluorescent molecules and the reactive groups available with these. The names and spectroscopic characteristics are listed in the table

CHAPTER 2 SYNTHESIS AND CHARACTERIZATION OF FLUORESCCEIN ISOTHIOCYANATE LABELED POLY(STYRENESULFONATE SODIUM SALT)

2.1 INTRODUCTION

Since the “extraordinary behavior” of polyelectrolyte in salt-free or low-salt solutions was discovered by Lin, S. C.²⁵ in 1978, the correct interpretation of this phenomenon has been debated for more than a quarter century. So far, most studies were done by dynamic light scattering (DLS); however, the scattering of visible light from polyelectrolyte solutions at low ionic strength is so weak that long acquisitions are required to get a reliable DLS signal. That means the dust or undissolved bits of polymer can corrupt the measurement. Compared with light scattering, Fluorescence Photobleaching Recovery (FPR) is expected to provide crucial information about transport behavior of the molecule and any aggregates. Unlike mutual diffusion coefficient gotten from DLS, FPR measures the optical tracer self diffusion coefficient which does not reflect the thermodynamic interaction. Therefore, FPR is an easily repeatable approach that provides new insight about the dynamic properties of polyelectrolyte in low-salt or salt-free solutions.

Pseudolinear and regularly branched water-soluble macromolecules are commercially available in fluorescently labeled form; these include dextrans and poly(amidoamine) dendrimers. The same is not true for the most commonly chosen example, poly(styrenesulfonate) sodium salt (NaPSS), which is a linear strong polyelectrolyte. The commercial NaPSS is produced by sulfonating polystyrene under harsh conditions;^{49, 50} however, it still may not be possible to achieve 100% degree of

sulfonation.^{51, 52} The residual hydrophobic patches along the chains may group together, leading to aggregation.⁵³⁻⁵⁵ There are some other concerns involved in the NaPSS synthesis and processing: the freeze-drying may give rise to more aggregates;^{56, 57} the filtering may remove the aggregates or domains;^{58, 59} and the contact with trace amounts of hydrophobic substances may be responsible for the slow mode.⁶⁰ Another problem is how to prepare NaPSS for the FPR measurement. The commercial NaPSS lacks highly reactive functional groups that would permit the direct attachment of fluorescein or its derivatives. In the 1990's, a two-step synthesis path was developed: chlorinate the sulfonate group in a $\text{PCl}_3/\text{POCl}_3$ mixture or pure POCl_3 , and then attach the fluoresceinamine.⁶¹ Because of the poor solubility of NaPSS in $\text{PCl}_3/\text{POCl}_3$ and POCl_3 , this heterogeneous reaction may result in uneven chlorination leading to uneven distribution of labeling. This will give rise to hydrophobic patches along the NaPSS chains.

To address these issues, a new strategy was developed to synthesize the fluorescein isothiocyanate (FITC) labeled NaPSS. A virgin NaPSS sample is directly co-polymerized from monomeric styrenesulfonate sodium salt and FITC-labeled 4-aminostyrene via atom transfer radical polymerization (ATRP). This monodispersed NaPSS has 100% degree of sulfonation and no hydrophobic defects. No drying procedure was involved during the polymerization, and the material does not come into contact with hydrophobic impurities. Dialysis centrifuge result and fluorescence spectra show that the FITC was successfully attached to the polymer. The diffusion of this labeled samples could be studied by FPR.

2.2 EXPERIMENTAL

2.2.1 MATERIALS

4-styrenesulfonic sodium salt, 4-vinylaniline (97%), fluorescein isothiocyanate isomer I (FITC), copper(I) chloride (99.995+%), 2,2'-bipyridine (99+%) (bpy), and deuterium oxide (D₂O) were purchased from Aldrich. Bromo-*p*-toluic acid (97%) (BPT) was purchased from Acros Organic. Silica Gel (63-200 nm particle size, 60 Å pore size) was purchased from Scientific Adsorbents Inc. Methanol (anhydrous) and tetrahydrofuran (THF) were purchased from Fisher Scientific. Molecularporous membrane tubing was purchased from Spectrum Laboratories, Inc.. Nanopure water (> 18.0 MΩ cm, Barnstead) was used throughout the experiment. All chemicals were used without further purification.

2.2.2 SYNTHESIS OF FITC-LABELED 4-AMINOSTYRENE

FITC 38mg (0.1 mmol) and 200 proof ethanol (8 mL) were added into a round-bottom flask. The solution was stirred, and a condenser and septa were connected to the flask. N₂ was introduced to the solution through a bubbler. Then 10

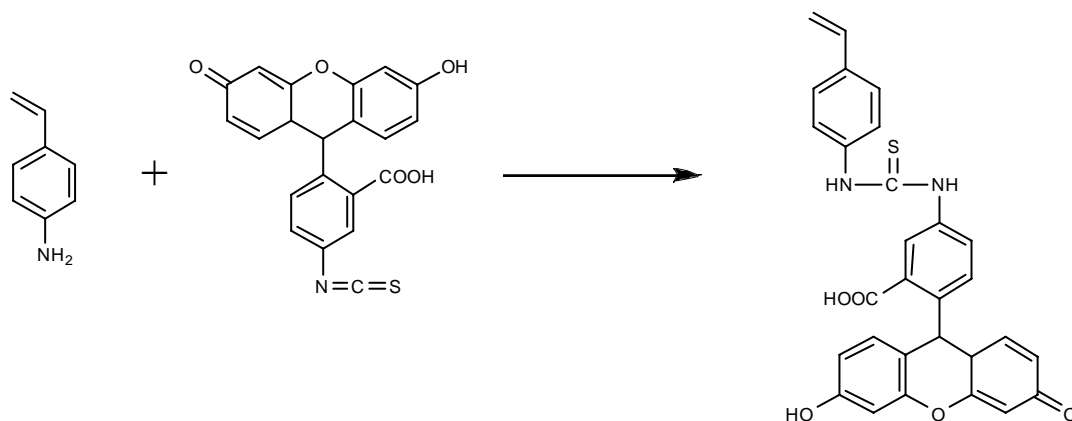


Figure 2.1 Reaction scheme for FITC-labeled 4-aminostyrene

mg (0.09 mmol) of 4-aminostyrene and 38 mg (0.10 mmol) were added to this solution under N₂ atmosphere. The use of excess FITC is designed to facilitate the labeling reaction. The reaction mixture was conducted at 50°C for 1 hour. The reaction was carried out for 24 hours at room temperature. 0.0825g solid, including product and unreacted dye, was gotten after rotary evaporation. A schematic regarding the synthesis is illustrated in Figure 2.1.

2.2.3 SYNTHESIS OF POLY(STYRENESULFONATE SODIUM SALT)

The “patchless” NaPSS was synthesized through atom transfer radical polymerization (ATRP) as described by S. P. Armes.⁶² 50 mL of Nanopure water and 50 mL of methanol were degassed with filtered N₂ for 30 minutes. 4.89g (21.3 mmol) of 4-styrenesulfonic sodium salt was first dissolved in 22 ml degassed Nanopure water in a round-bottomed flask. 51 mg (0.24 mmol) of initiator, BPT, was added into the solution and the pH was adjusted to 10~11 with 1M NaOH (~1.2 ml) so as to just completely dissolve the initiator. 6 mL of degassed methanol was added to the solution. Then this solution was purged with filtered N₂. After 30 minutes, 24 mg of copper(I) chloride (0.24 mmol; 1 equiv.) and 74 mg of bpy (0.48 mmol; 2 equiv.) were added in solution while maintaining a slow N₂ purge. The reaction solution turned to brown and was stirred at the room temperature. After 48 hours, the reaction was stopped by opening the flask to air. 5 mL anhydrous methanol and 5 mL Nanopure water were added into the reaction solution. The solution turned to blue after about 30 minutes. The product was checked by adding several drops of solution

into methanol. Some white precipitate was seen.

The reaction solution then was purified through a silica gel column to get rid of the copper ions. A mixture solute (methanol/Nanopure water = 28ml/100ml) was used to wash the column until no polymer can be gotten from the eluate. The product was obtained by rotary evaporation, and the final yield was 98%. This sample was purified at least three times by dissolving in water and then precipitating with methanol before the GPC grading.

2.2.4 SYNTHESIS OF POLY(FITC-LABELED AMINOSTYRENE-CO-STYRENESULFONATE SODIUM SALT)

The protocol of poly(FITC-labeled aminostyrene-*co*-styrenesulfonate sodium salt) synthesis is fundamentally the same as that used for the virgin NaPSS synthesis. All of the FITC-labeled aminostyrene prepared in 2.2.2 was dissolved in 5 mL methanol and degassed with filtered N₂ for 15 minutes. This solution was added into the reaction mixture by syringe after the step of adjusting the pH to 10~11. The reaction was conducted for 44 hours at the room temperature. After purified through a silica gel column, the eluate was bright yellow. A yellow precipitate was resulted when several drops of this eluate was added to methanol. A light brown product was

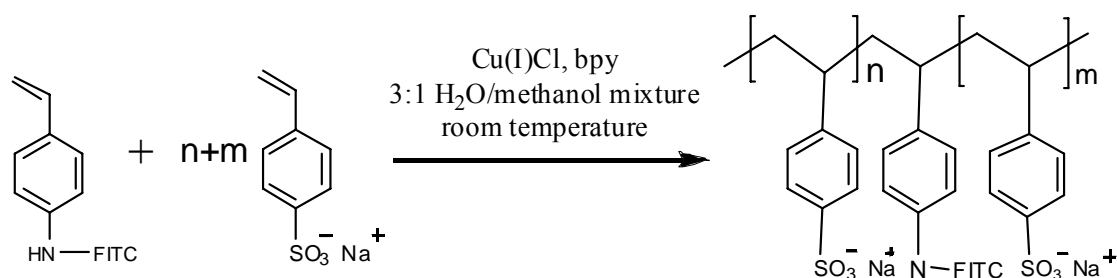


Figure 2.2 Reaction scheme for the polymerization of poly(FITC-labeled aminostyrene-*co*-styrenesulfonate sodium salt)

obtained by rotary evaporation, and the final yield is 97.7%. Preparation of the poly(FITC-labeled aminostyrene-*co*-styrenesulfonate sodium salt) is shown in Figure 2.2.

2.2.5 PURIFICATION OF POLY(FITC-LABELED AMINOSTYRENE-CO-STYRENESULFONATE SODIUM SALT)

Poly(FITC-labeled aminostyrene-*co*-styrenesulfonate sodium salt) (2.68 g) was dissolved in 50 mL Nanopure water and stirred for 30 minutes. During this time, a dialysis tube (Spectra/Pro Membrane, MWCO=3,500) was boiled in Nanopure water for 15 minutes. Then the solution was added into this dialysis tube, and the tube was put in a 2-liters beaker which was fully filled with Nanopure water and stirred with a magnetic bar. The dialysis water was changed for every 2 hours for the first 6 hours and then changed for every 6 hours. The dialysis effect was checked after 2 days and 4 days: 0.3 ml dialyzed solution was added in Microcon (MWCO=3,000) and centrifuged for 30 minutes at 10000 RPM (g-field= 12000); the solution in the lower layer was then tested for the absence of free dye by visual observation in a 488 nm laser. No free dye could be seen after 4 days dialysis.

2.2.6 CHARACTERIZATION

- **Molecular Weight Distribution.** The molecular weight and polydispersity index were obtained by GPC/MALLS using a Wyatt multiangle light scattering (DAWN HELEOS) and quasielastic light scattering (QELS) instrumentation along with an Optilab rEX differential refractometer and ASTRA V software. The specific refractive index increment, dn/dc , was taken as 0.198 mL/mg.⁶³ The GPC column was PL

Aquagel-OH mixed 8 μm (Polymer Laboratories). Samples were dissolved in the mobile phase, 200 mM NaNO_3 + 10 mM NaH_2PO_4 + 2 mM NaN_3 , adjusted to pH 7.5. The injected volume was 0.10 mL, and the flow rate was 0.5 mL/min. The weight-average molecular weight and its standard deviation were calculated from three or more repeat measurements. In estimating R_g , a random coil model was selected in the Wyatt Astra software.

- **^1H NMR Spectra.** ^1H NMR spectra were acquired on a Bruker APX 300 spectrometer at 25°C with a 90° pulse of 6.95 μs . 5 w% of product was dissolved in D_2O for 48 hours before NMR measurement. The extraordinary amount of product was designed to highlight the trace of FITC dye.
- **Fluorescence Spectroscopy.** Fluorescence spectra were recorded with Perkin-Elmer luminescence spectrophotometer LS 50B. A quartz cuvette with 1-cm path length was used. Nanopure water was adjusted to pH \sim 7.5 with 1.0 M NaOH/HCl , and labeled NaPSS was dissolved in this solute to prepare 0.5 mg/mL sample. The scanned wavelength was from 350 nm to 600 nm.
- **FPR Measurement.** The FPR apparatus has been described in chapter 1. The striped pattern was created by illuminating a coarse diffraction grating (Ronchi ruling), which was held in the rear image plane of a standard epifluorescence microscope, with an intense, brief laser flash. An electromechanical modulation detector system monitors the subsequent disappearance of the pattern due to the exchange of molecules that were bleached and those that were not. The contrast signal (AC amplitude) from the modulation detector decays exponentially:

$$C(t) = \exp(-K^2Dt) \quad (\text{Eq. 2.1})$$

Where the spatial frequency of the grating is $K = 2\pi/L$, with L representing the distance between the same side of adjacent stripes in the Ronchi ruling, and D is the optical tracer self-diffusion coefficient. Twelve different K values can be used to verify to absence of nondiffusive signal recovery, which could result in finite recovery rates even at $K=0$. In this work, most runs were performed in triplicate at a single K value.

2.3 RESULTS AND DISCUSSION

2.3.1 FITC-LABELED 4-AMINOSTYRENE

Figure 2.3 is the mass spectrometry analysis of FITC-labeled aminostyrene. It shows a sharp peak at 509.1171 m/z corresponding to the molecular weight of FITC-labeled aminostyrene, 508.48. The difference between these two values is assigned as the mass of a proton which loads charge on this molecule. The other peaks, 348.0314, 390.1462, and 436.0849, are considered to be the fragments and the free FITC dye (MW= 389.38).

2.3.2 UNLABELED NAPSS AND FITC-LABELED NAPSS

An analysis of the virgin NaPSS, FITC-labeled NaPSS and commercial NaPSS is shown in Figure 2.4 with the means of ^1H NMR. All of the NMR spectra show the feature peaks at 1~2 ppm and at 6~8 ppm, which corresponding to the backbone and aromatic ring of NaPSS, respectively. The peak at 4.6 ppm in Figure 2.4 (a) is

assigned to residual H₂O.

Unfortunately, the amount of labeled aminostyrene incorporated is too low to be precisely characterized by ¹H NMR. No ¹H peak from aminostyrene or FITC appeared in the ¹H NMR spectrum because of the low content of these groups. Based on the ratio of reagent feed, an upper bound of FITC content can be estimated: the percentage of FITC-labeled aminostyrene in poly(FITC-labeled aminostyrene-*co*-styrenesulfonate sodium salt) is less than 0.7 mol %. The percentage of styrenesulfonate sodium monomers in poly(FITC-labeled aminostyrene-*co*-styrenesulfonate sodium salt) must be > 99%, which exceeds the degree of sulfonation achieved by most commercially available NaPSS.

Table 2.1 lists the characterization results for virgin NaPSS, FITC labeled NaPSS and commercial NaPSS. The ATRP approach leads to narrow polydispersity indexes for virgin NaPSS and FITC labeled NaPSS, 1.11 and 1.07 respectively. Those polydispersity indexes are much better than that of bulk commercial NaPSS. The molecular weights of virgin NaPSS and FITC-labeled NaPSS are close to each other. It indicates that there is no obvious effect of FITC-labeled aminostyrene on the polymerization. The GPC/MALLS traces are shown in Figure 2.5. An impurity peak was observed in the dRI trace for both labeled and unlabeled product. Some measurements were carried out to look for the origin of this impurity. A same peak was finally found in the dRI trace of monomer. Therefore, the dRI trace of labeled and unlabeled NaPSS were normalized by abstract the impurity peak. Figure 2.5 (a) and (b) present the GPC trace in order of dRI of monomer, dRI of product before

normalization, dRI of product after normalization, and LS of product. Figure 2.6 shows the M and root mean square (RMS) radius plot of FITC-labeled NaPSS and unlabeled NaPSS.

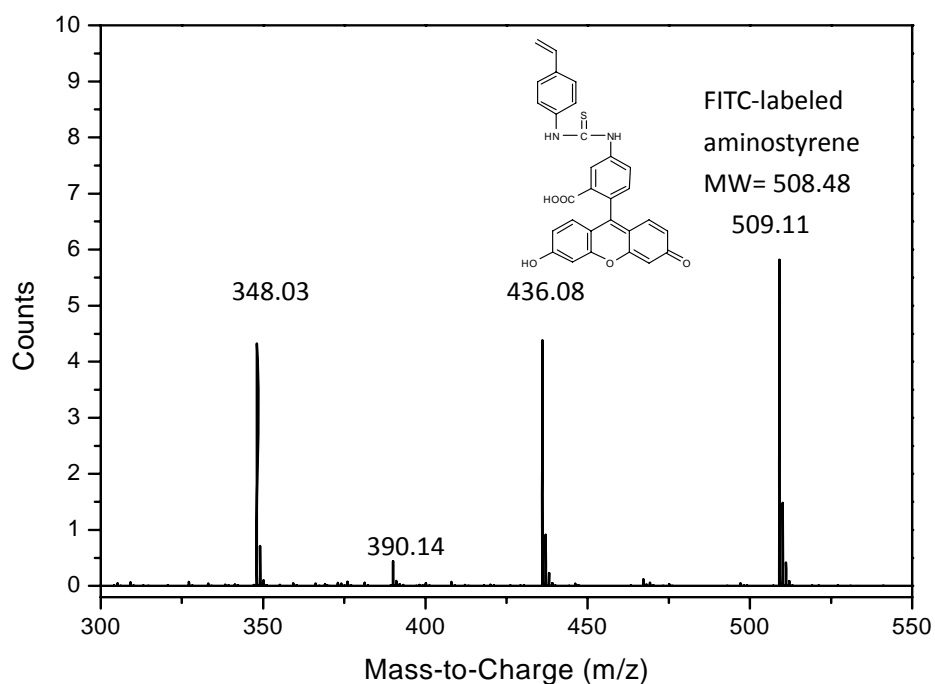


Figure 2.3 Mass spectrometry analysis of FITC labeled 4-aminostyrene

Table 2. 2 Characterization of virgin NaPSS, FITC-labeled NaPSS, and commercial NaPSS with GPC/MALLS

Product	4-styrenesulfonate sodium salt (g)	FITC-labeled aminostyrene (g)	M_w	PDI M_w/M_n
Unlabeled NaPSS	4.89	0	129,000±600	1.110±0.003
FITC-labeled NaPSS	4.89	0.0875	148,000±600	1.071±0.002

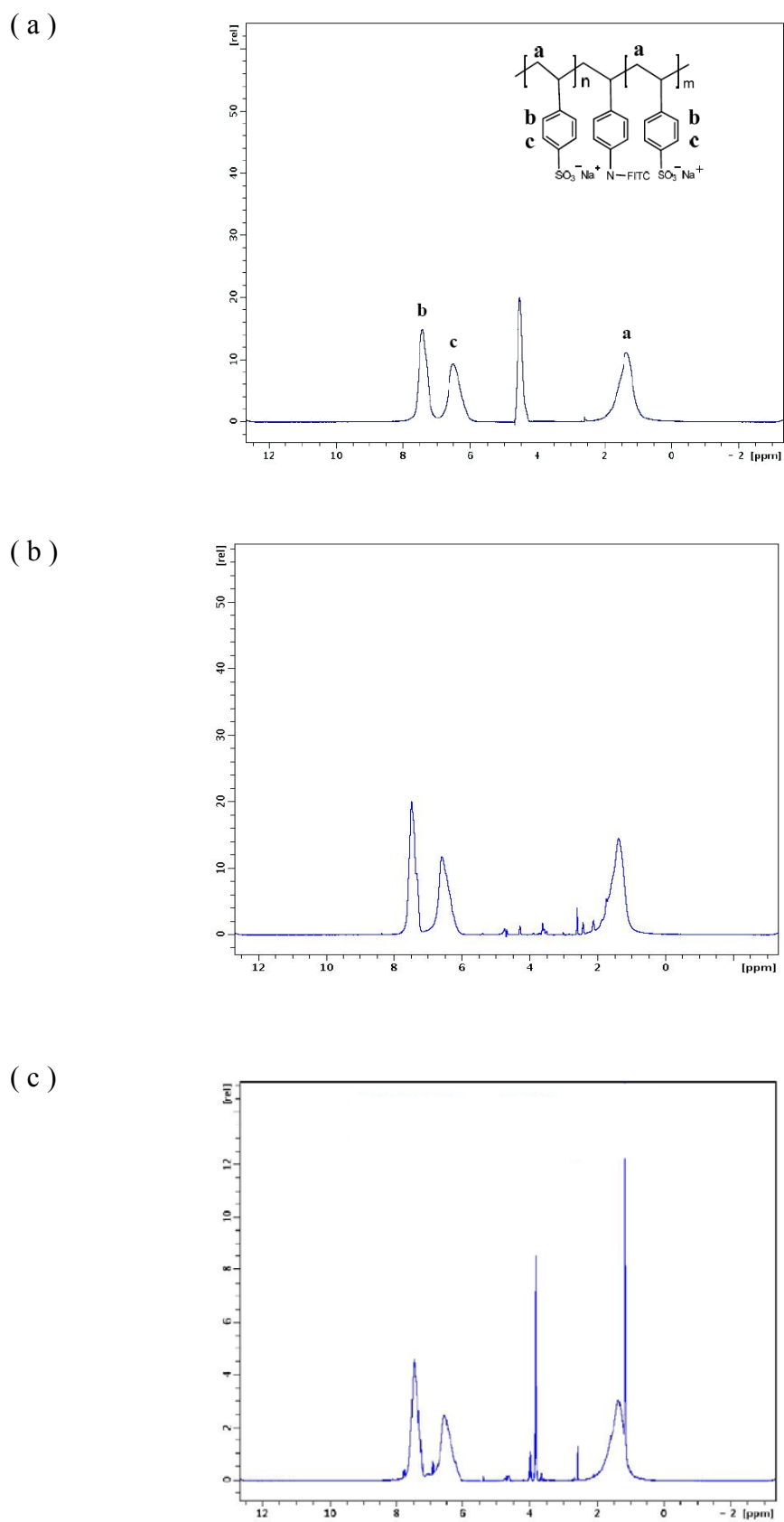


Figure 2. 4 ^1H NMR spectra for: (a) FITC-labeled NaPSS, (b) virgin NaPSS, (c) commercial NaPSS

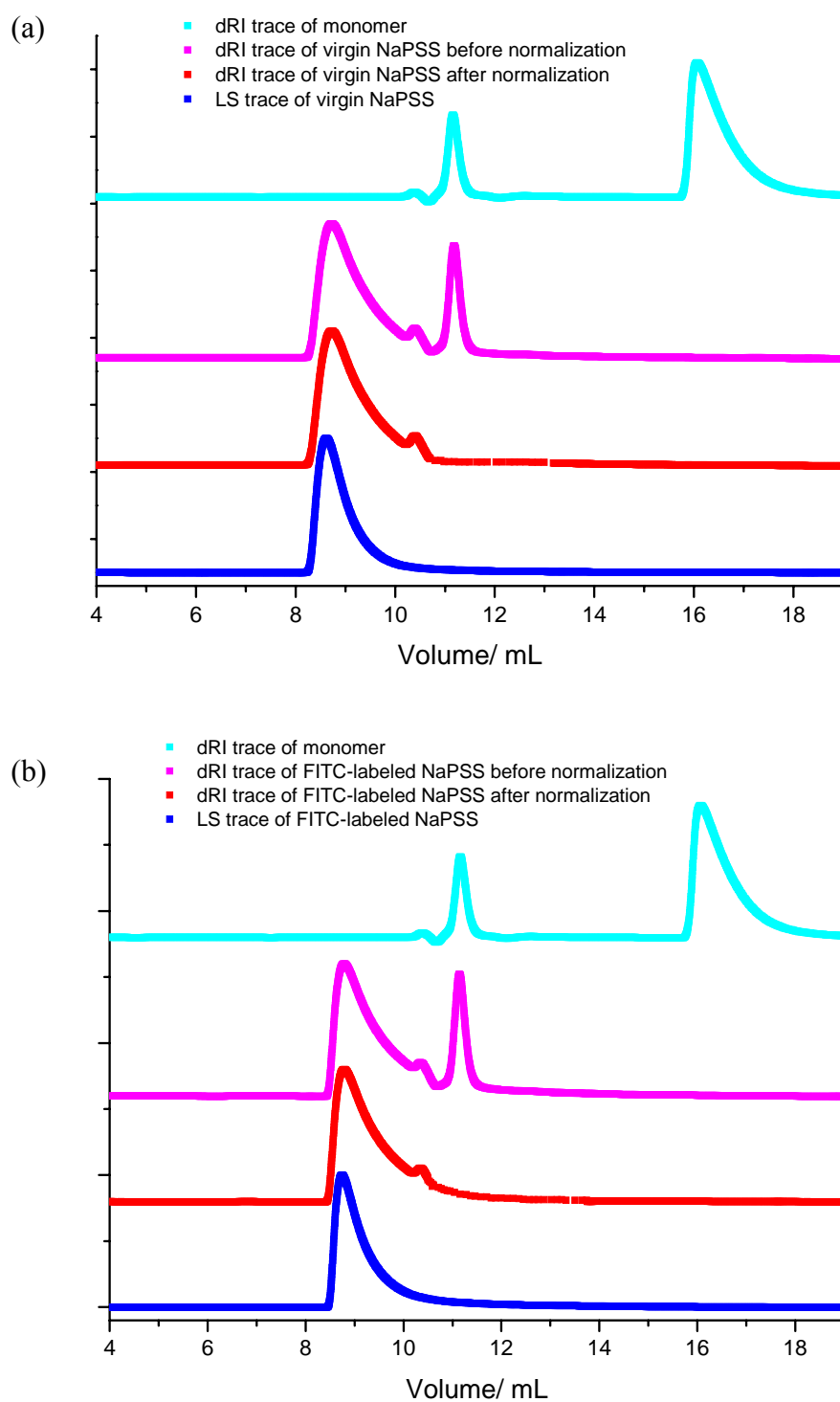


Figure 2. 5 GPC/MALLS traces for: (a)virgin NaPSS, (b) FITC-labeled NaPSS

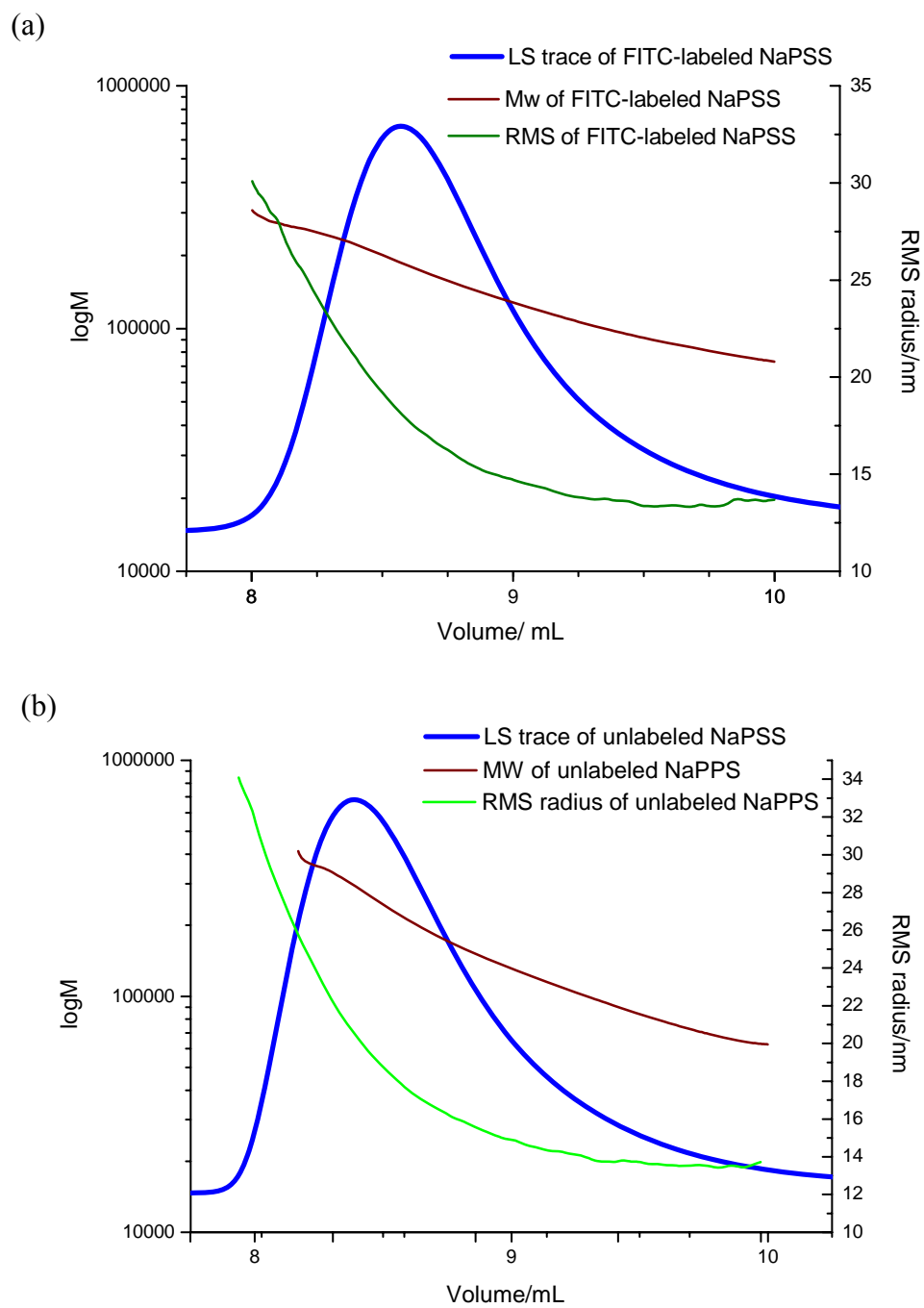


Figure 2.6 The M and RMS radius plot of (a) FITC-labeled NaPSS, (b) unlabeled NaPSS

2.3.3 FLUORESCENCE PROPERTIES OF POLY(FITC AMINOSTYRENE-CO-STYRENESULFONATE SODIUM SALT)

The presence of FITC in poly(aminostyrene-co-styrenesulfonate sodium salt) was indicated by the yellow color of solution, which had been dialyzed after 4 days. The dialysis result was also checked by centrifuge: 0.3 mL solution from dialysis tube was added in a Microcone (MWCO=3000) and centrifuged at 10000 RPM (g-field = 11950) for 30 minutes. Figure 2.7 shows the lower lay solutions in the Microcone after centrifuge. The eluent did not appear colored any more after the sample was dialyzed for 4 days. It also hardly can see any fluorescence in this eluent under the illumination of blue laser light. Then the sample solution was rotary evaporated. Figure 2.8 shows the FITC-labeled NaPSS still looks bright yellow after 4 days dialysis. The successful attachment of FITC was later confirmed by fluorescent spectrum analysis. Figure 2.9 shows the fluorescence spectra of FITC-labeled NaPSS at pH 7.5. The positions of excitation peak and emission peak are 492 nm and 518 nm, respectively. They are in good agreement with those of recorded fluorescein spectra, which with the maximum excitation and emission wavelength at 494 nm and 520 nm at pH 8.0.

The level of dye labeling was estimated by calculating the FITC concentration in sample solution. The fluorescence calculation was produced with pure FITC solutions at pH 9.5. The maximum excitation and maximum emission wavelengths were set at 494 nm and 514 nm, respectively. Table 2.2 shows the experimental data and calculation result for FITC-labeled NaPSS. The calculation result suggests that about four FITC group attached to per ten thousand styrenesulfonate monomer. If taking the

weight average molecular weight into account, only one fourth polymer chains are singly tagged. Therefore, intramolecular associations between the dye units are unlikely to alter the conformation.

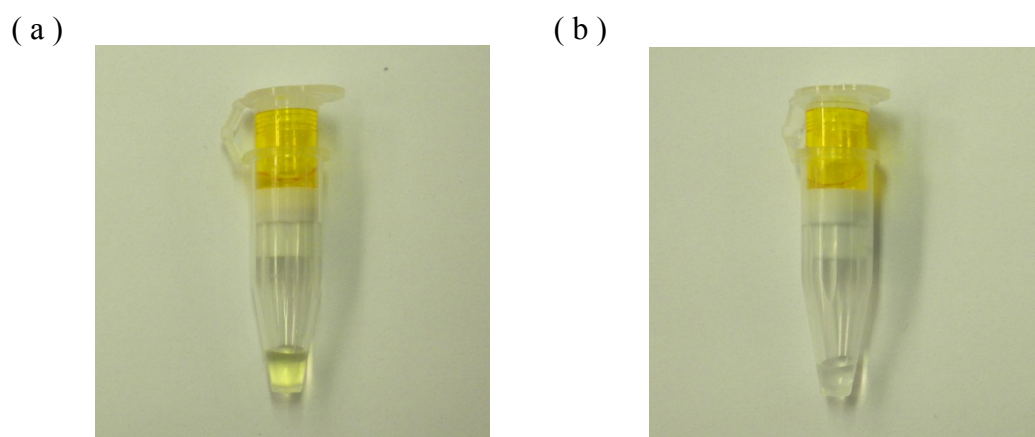


Figure 2. 7 The low layer solutions in Microcone after dialysis and centrifuge: (a) dialyzed for 2 days, (b) dialysis for 4 days. Both solutions have been centrifuged at 10000 RPM (g-field=11950) for 30 minutes.

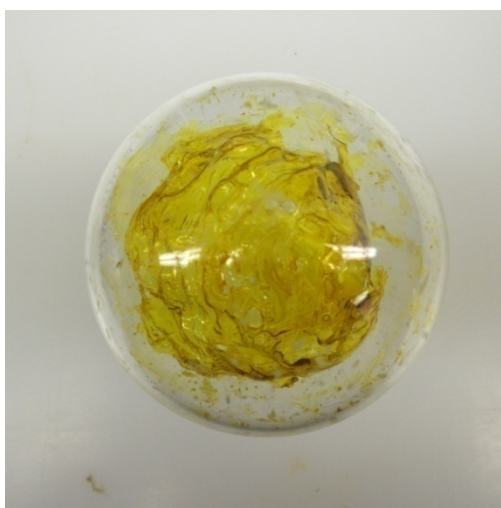


Figure 2. 8 FITC Labeled NaPSS after 4 days dialysis and rotary evaporation

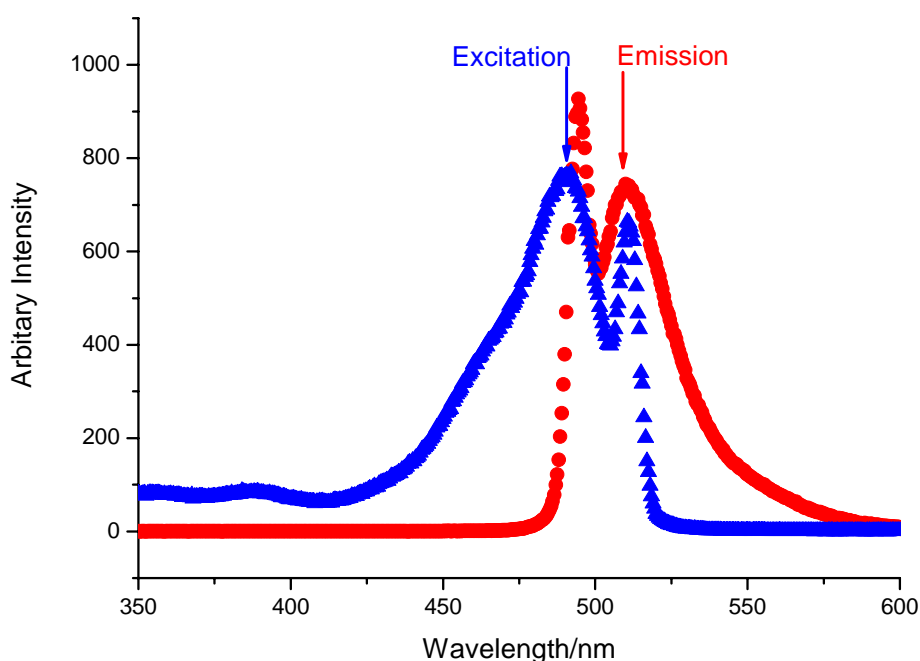


Figure 2. 9 Fluorescence spectra for FITC-labeled poly(styrenesulfonate sodium salt). The sample was dissolved in Nanopure water, which pH was adjusted to ~7.5 with 0.01 M NaOH/HCl. Emission wavelength: 518 nm. Excitation wavelength: 492 nm.

Table 2. 2 The level of dye labeling for FITC-labeled NaPSS

Sample	Conc. (mg/mL)	FITC conc. (mg/mL)	FITC/styrenesulfonate monomer (mol/mol cal)	FITC/NaPSS (mol/mol cal)
FITC-labeled NaPSS	0.05	0.045	0.000373	0.25

2.3.4 GPC FRACTIONS OF FITC-LABELED NAPSS

For the study of polyelectrolytes in salt-free or low-salt solutions, the most controversial topic is the interpretation of slow mode diffusion. Some researchers assigned it to the complicated interactions between charged polymer chains; while the others considered it to be a result of clusters or aggregations. Most investigations have been devoted to this area, but the prospect is still obscure. It has been observed that

the slow mode diffusion is related with the molecular weight of polyelectrolyte (Figure 1.5). A series of monodispersed polyelectrolytes with different molecular weight will greatly facilitate the study of dynamic properties.

The FITC-labeled NaPSS were separated with the means of analytical scale GPC. Twelve fractions were collected in vials after a single injection of 0.6 mg (0.6 % solution×0.1 ml). Although the fractions were diluted in the GPC too low to appear yellow color, each fraction was fluorescent in the illumination of blue laser light. Table 2.3 shows the GPC analysis of the original samples and fractions. The molecular weights of fraction 1 and fraction 12 are opposite with the trend of other molecular weight change. These errors are probably due to the inaccuracy of calculation; the eluate is too diluted at the outer wings of the GPC peak.

2.4 CONCLUSIONS

Poly(FITC-labeled aminostyrene-*co*-styrenesulfonate sodium salt) was synthesized through atom transfer radical polymerization (ATRP). This FITC-labeled copolymer has molecular weight at 137,000 and a narrow polydispersity index at 1.071 which due to the living features of ATRP. This product was dialyzed for 4 days until no more free dye could be washed off by centrifugal dialysis. The sample after dialysis appears bright yellow color and still shows typical fluorescence emission/excitation behaviors. This FITC labeled copolymer was then separated into twelve fractions by analysis scale GPC. All of these fractions were characterized by GPC/MALLS.

Table 2.3 Characterization of virgin NaPSS, FITC-labeled NaPSS, and FITC-labeled NaPSS fractions by GPC/MALLS

Product (L=FITC-labeled)	<i>M_w</i>	PDI <i>M_w/M_n</i>	<i>D/10⁻⁷</i> <i>cm²s⁻¹</i>
1	129,000±260	1.11	-----
L2	148,000±148	1.07	6.01±0.23
L2-GPC fraction 1	75000±600	1.095	
L2-GPC fraction 2	191,000±380	1.011	
L2-GPC fraction 3	186000±190	1.002	
L2-GPC fraction 4	159000±160	1.002	
L2-GPC fraction 5	138,000±280	1.001	2.10±0.214
L2-GPC fraction 6	121,000±240	1.001	2.31±0.263
L2-GPC fraction 7	107,000±210	1.001	2.66±0.375
L2-GPC fraction 8	96,000±200	1.001	3.03±0.58
L2-GPC fraction 9	87,000±170	1.000	3.16±0.634
L2-GPC fraction 10	76,000±150	1.009	3.37±0.668
L2-GPC fraction 11	58,000±290	1.003	
L2-GPC fraction 12	107,300±540	1.054	

CHAPTER 3 OPTICAL TRACER DIFFUSION STUDIES OF POLYELECTROLYTE SOLUTIONS

3.1 INTRODUCTION

Among those complex and not yet understood properties of polyelectrolyte in solution, the presence of extraordinary transition of polyelectrolyte in low-salt or salt-free solutions is most intensively discussed since they were first discovered by Schurr and his co-workers. A very slow diffusion mode of poly-L-lysine in low salt range was reported.²⁵⁻²⁷ Later, more investigations indicate^{5-7, 10, 28-30} that such a “slow mode” is universal for essentially all investigated polyelectrolytes.^{31, 32} So far, this phenomenon has been attributed to different origins. Schmitz³⁹ proposed an idea that the fast mode diffusion is related to the coupled diffusion of polyelectrolyte chains and their counterions. The counterions around a parent polyion chain are dense and asymmetric. They diffuse very fast and result in electric field fluctuations. The polyion chains are trapped by this fluctuation which induces an electrophoretic mobility-related diffusive relaxation. For the slow mode diffusion, the proposed interpretation is even more interesting but controversial. It has been attributed to the dynamics of large, multi-chain domains or some insoluble chain clusters or even a defect from the thermal history during the imperfect processing of the polyelectrolyte samples.

Most of these polyelectrolyte investigations were conducted by means of the dynamic light scattering (DLS) technique. For the neutral polymers or polyelectrolytes in high salt solutions, diffusion coefficients could be calculated from

the characteristic decay times which were gotten from the DLS experiment. For the polyelectrolytes in low-salt or salt-free solution, however, the situation is more complicated. The scattering intensity of polyelectrolytes becomes very weak when they are in low-salt or salt-free solutions. This greatly deteriorates the accuracy of experimental data. Although recently, the advanced computer and detector techniques enable us to conduct better measurements, the preparation of a dustless sample for the long acquisition times required by the low scattering intensity is still painful.

Fluorescence Photobleaching Recovery (FPR) is a technique that relies on labeling the polymer chain with a photochromic dye. It is a more convenient and less controversial diffusion detector than DLS. Hundreds of runs could be done with several microlitter samples in one hour. In contract to DLS, FPR obtains the optical tracer self diffusion coefficient and usually obtains diffusion on longer time and distance scales.

The partial specific volume of charged macromolecule in solution provides a bridge connecting weight fraction (wt/wt), concentration (wt/vol), and volume fraction (vol/vol). It is of importance in the interpretation of polyelectrolyte diffusion. The partial specific volume can be determined experimentally through density measurement. Since the partial volumes can be looked upon as the sum of the true volumes of the ions themselves and of the associated volume changes of the solvent, a solute-solvent interaction is required.

In this study, the densities of various NaPSS concentrations in both aqueous solution and salt solution were examined. A FPR device is also used to investigate the

translational diffusion of labeled NaPSS in aqueous solutions

3.2 METHODS

Density measurements were carried out at 20°C using a Paar DMA 58 densitometer. Calibrations were performed with water and at least one calibration standard for every different concentration. Commercial NaPSS ($M_w=70,000$, $PDI=1.1$) sample was dissolved in Nanopure water and 10 wt% NaCl solution, respectively, for 4 days before measurement. Every density value was estimated from three runs.

The FPR apparatus has been described in chapter 1. The striped pattern was created by illuminating a coarse diffraction grating (Ronchi ruling) held in the rear image plane of a standard epifluorescence microscope with an intense, brief laser flash. An electromechanical modulation detector system monitors the subsequent disappearance of the pattern due to exchange of molecules that were bleached and those that were not. Figure 3.1 shows the program screen of FPR software. The white dotted line represents the DC amplitude which is the intensity of the illumination light; the green dots represent the AC amplitude which indicates the decay of the contrast in the bleached strip pattern; the green dotted line is the baseline estimated from the AC amplitude before bleaching. The contrast signal (AC amplitude) from the modulation detector decays exponentially:

$$C(t) = \exp(-K^2Dt) + B \quad (\text{Eq. 2.1})$$

where the spatial frequency of the grating is $K = 2\pi/L$, with L representing the spatial period projected by the Ronchi ruling into the sample, D is the optical tracer

self-diffusion coefficient, and B is the baseline. The experimental data were fitted by Anscan. Figure 3.2 is the stimulation screen of Anscan. Many different K values can be used to verify the absence of nondiffusive signal recovery, which could result in finite recovery rates even at $K=0$. Most runs were performed in triplicate at a single K value.

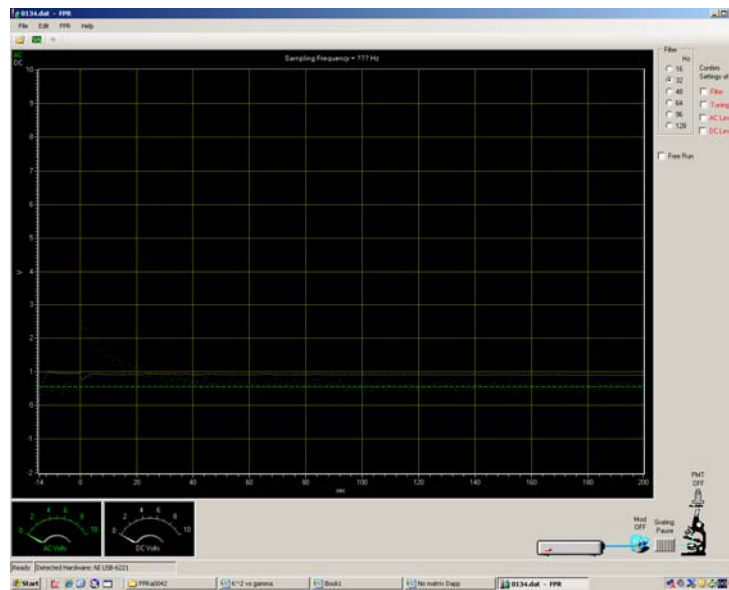


Figure 3. 1 The windows of FPR program. White spot line: DC amplitude; green spots: AC amplitude; green spot line: baseline.

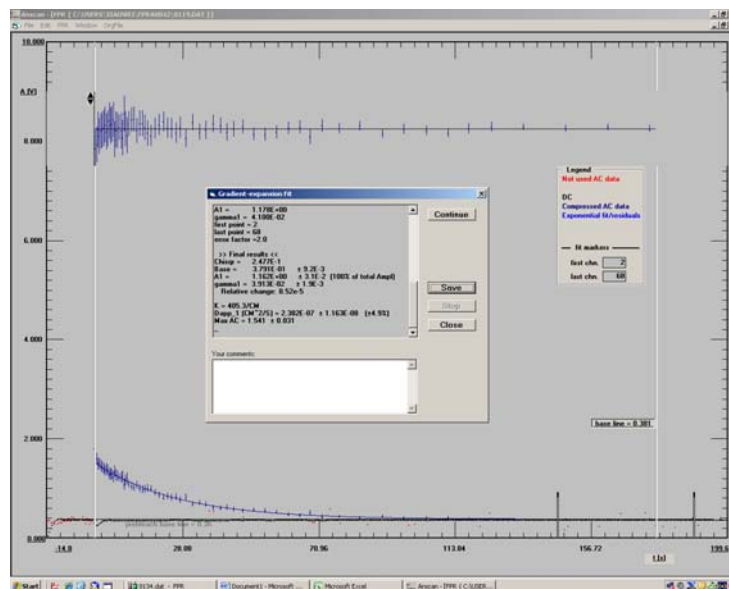


Figure 3. 2 The windows of Anscan. The internal window is showing the stimulation result calculated by the program.

3.3 RESULTS AND DISCUSSION

3.3.1 DENSITY OF NAPSS SOLUTION

The partial specific volume, \tilde{v} , of the solute is defined as the change in total volume, ∂V , per unit mass upon adding an infinitesimal amount, ∂g_2 , of the solute at constant temperature, T , pressure, p , and composition of the components.

$$\tilde{v} = \left(\frac{\partial V}{\partial g_2}\right)_{T,p,n}$$

The partial molar volume, \bar{V} , is defined in an analogous way by substituting the number of solute grams, g_2 , by the number of solute moles, n_2

$$\bar{V} = \left(\frac{\partial V}{\partial n_2}\right)_{T,p,n}$$

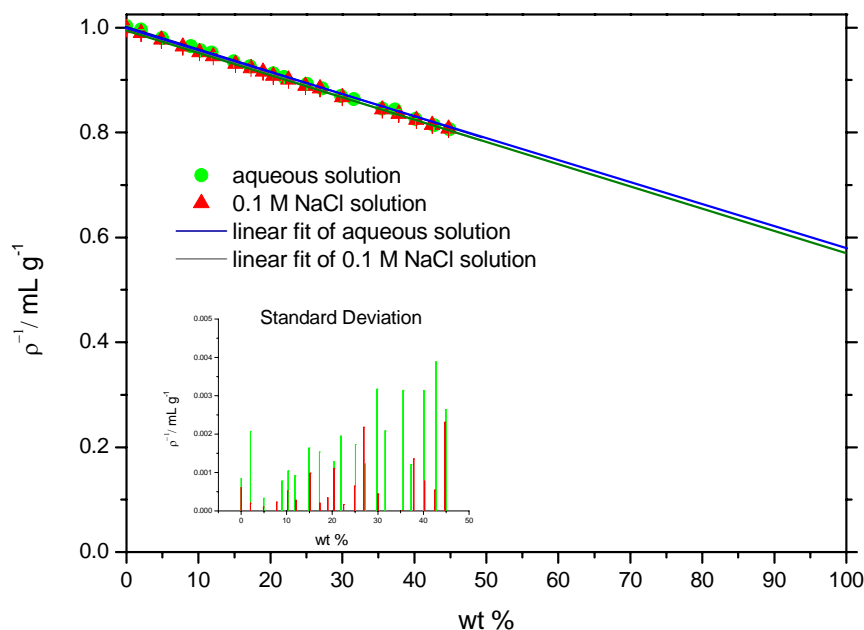


Figure 3. 3 Inverse of density dependence of the weight fraction for the aqueous solution and salt solution of commercial NaPSS ($M_w=70,000$, $PDI=1.1$). The interior graph is the standard deviation for the experimental data and the fitted linear.

As it is hard to know the precise molecular weight of polymer, the partial specific volume is more commonly measured by macromolecular scientists than the partial mole volume.

Figure 3.3 shows the inverse of the solution density (i.e., $V/(g_1+g_2)$) against weight fraction of solute (i.e., $g_2/(g_1+g_2)$). It indicates that both the partial specific volumes of NaPSS in aqueous solution and in 0.1 M NaCl salt solution are independent with NaPSS concentration. The partial specific volume of NaPSS in aqueous solution and salt solution is 0.5743 ± 0.0002 and 0.5637 ± 0.0004 , respectively.

3.3.2 SELF-DIFFUSION OF GPC FRACTIONS WITH FPR

For the self-diffusion study, all of the fractions in the GPC eluent were sealed in FPR rectangular cells (0.3×3.0 mm I.D., VistroCom) and measured with four different K value, including $K=157$, 253, 405.3, and 583 cm^{-1} . Only fractions 5 to 10 have accurate relations between diffusion coefficient and the corresponding molecular weight. The rest fractions behaved weird which mostly came from the shoulder of GPC peak. This is probably due to their too diluted concentration. Figure 3.3 shows gamma versus K^2 for fractions 5, 7, and 8. The experimental data when K is at 405.3 and 583 cm^{-1} is more acceptable than the other data. Since light labeling and very low concentration, the data measured when K is at 157 and 253 cm^{-1} is too noisy to be processed.

The diffusion coefficients and molecular weight of fraction 5 to fraction 10 are presented in Table 3.1. It is clear that the self-diffusion increase with the decrease of

molecular weight. The uncertainty in D is higher than the several percent we have come to expect of FPR in aqueous systems due to the very low concentrations. The range of M values explored is not very wide, but the observed power law slope of about $-3/5$ does meet the expectation for a screened polyelectrolyte chain; i.e., the polymer behaves as a random coil in a good solvent in this buffer (200 mM NaNO_3 +10 mM NaH_2PO_4 +2 mM NaN_3 adjusted to pH 7.5)

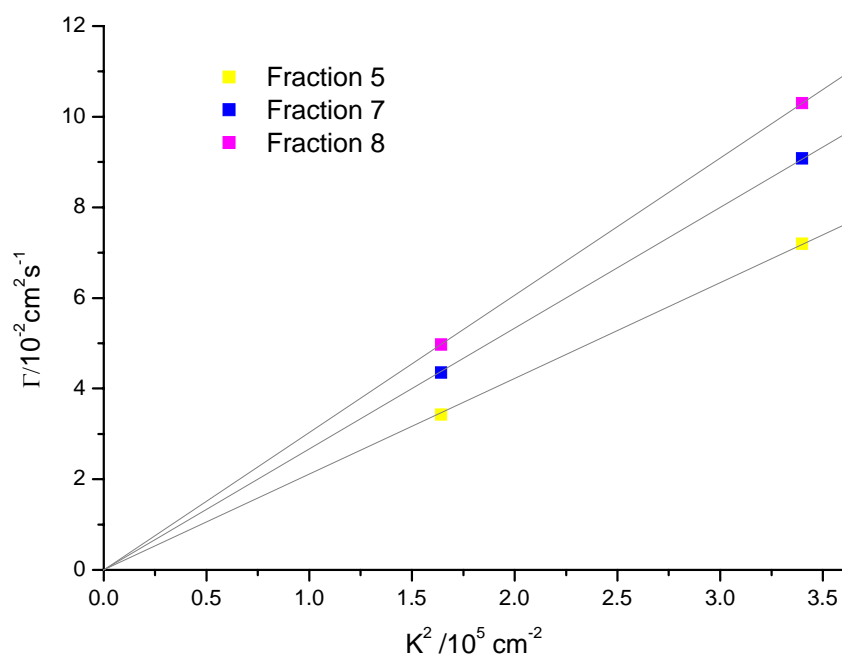


Figure 3.4 FPR result of Γ versus K^2 for fraction 5, 7, and 8

Table 3.1 Diffusion coefficients of fraction 5 to fraction 10. The result were calculation from the liner fit of Figure 3.3

	Fraction 5	Fraction 6	Fraction 7	Fraction 8	Fraction 9	Fraction 10
$D/10^{-7}$ cm^2s^{-1}	2.10 ± 0.21	2.31 ± 0.26	2.66 ± 0.37	3.03 ± 0.58	3.16 ± 0.63	3.37 ± 0.66
Mw	138,000 ± 280	121,000 ± 240	107,000 ± 210	96,000 ± 200	87,000 ± 170	76,000 ± 150

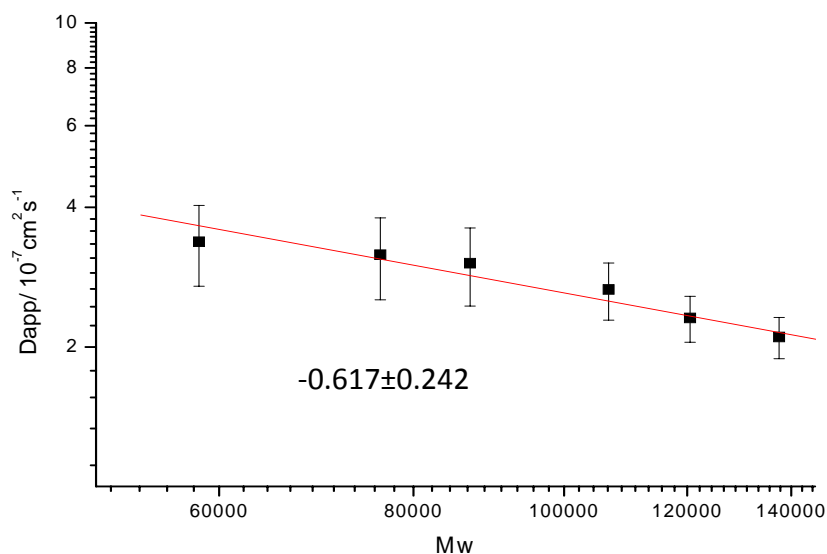


Figure 3. 5 Diffusion of FITC labeled NaPSS fractions obtained from GPC. The power law slope over the limited range of M_w available is indicated.

3.4 CONCLUSIONS

The density of various NaPSS concentration in both aqueous solution and salt solution were examined with densitometry. Both kinds of densities are independent of NaPSS concentration. There is no significant difference between the partial specific volume of NaPSS in aqueous solution and salt solution, meaning that the structures underlying the slow mode are not detectable by densitometry. The self-diffusion of the FITC labeled NaPSS fractions, collected from an injection through the analytical scale GPC/MALLS, were investigated with FPR. Although all of the fractions have obvious fluorescence photobleaching reaction, the behavior of fraction 5 to fraction 10 is more reasonable. Their diffusion coefficients were estimated by stimulating the function between Γ and K^2 . These graphs indicate that there is no free dye in the fraction solutions which gives rise to a diffusion even when $K=0$. These diffusions were plotted against the molecular weight. The slope is -0.617 , which is in good

agreement with power law. This indicates that the polyelectrolyte chains behave like a random coil in the GPC buffer.

REFERENCES

1. P. S. Russo, J. Q., Nadia Edwin, Young-wook Choi, Garrett J. Doucet, and Daewon Sohn, Fluorescence Photobleaching Recovery. In *Soft Matter: Scattering Imaging and Manipulation*.
2. Craig Pryor, James Donley, <http://valence4.com/protein.html>
3. Odijk, T. *Macromolecules* **1979**, 12, (4), 688-693.
4. Sedlak, M. *Langmuir* **1999**, 15, (12), 4045-4051.
5. Sedlak, M.; Amis, E. J. *Journal of Chemical Physics* **1992**, 96, (1), 817-825.
6. Koene, R. S.; Mandel, M. *Macromolecules* **1983**, 16, (6), 973-978.
7. Forster, S.; Schmidt, M.; Antonietti, M. *Polymer* **1990**, 31, (5), 781-792.
8. Drifford, M.; Dalbiez, J. P. *Journal De Physique Lettres* **1985**, 46, (7), L311-L319.
9. Drifford, M.; Dalbiez, J. P. *Journal of Physical Chemistry* **1984**, 88, (22), 5368-5375.
10. Mathiez, P.; Mouttet, C.; Weisbuch, G. *Biopolymers* **1981**, 20, (11), 2381-2394.
11. Maeda, T. *Macromolecules* **1991**, 24, (10), 2740-2747.
12. Ise, N.; Okubo, T.; Hiragi, Y.; Kawai, H.; Hashimoto, T.; Fujimura, M.; Nakajima, A.; Hayashi, H. *Journal of the American Chemical Society* **1979**, 101, (19), 5836-5837.
13. Ise, N.; Okubo, T.; Kunugi, S.; Matsuoka, H.; Yamamoto, K.; Ishii, Y. *Journal of Chemical Physics* **1984**, 81, (7), 3294-3306.
14. Ise, N.; Okubo, T.; Yamamoto, K.; Kawai, H.; Hashimoto, T.; Fujimura, M.; Hiragi, Y. *Journal of the American Chemical Society* **1980**, 102, (27), 7901-7906.
15. Williams, C. E.; Nierlich, M.; Cotton, J. P.; Jannink, G.; Boue, F.; Daoud, M.; Farnoux, B.; Picot, C.; Degennes, P. G.; Rinaudo, M.; Moan, M.; Wolff, C. *Journal of Polymer Science Part C-Polymer Letters* **1979**, 17, (6), 379-384.

16. Nierlich, M.; Williams, C. E.; Boue, F.; Cotton, J. P.; Daoud, M.; Farnoux, B.; Jannink, G.; Picot, C.; Moan, M.; Wolff, C.; Rinaudo, M.; Gennes, P. G. D. *Journal De Physique* **1979**, 40, (7), 701-704.
17. Nierlich, M.; Williams, C. E.; Boue, F.; Cotton, J. P.; Daoud, M.; Farnoux, B.; Jannick, G.; Picot, C.; Moan, M.; Wolff, C.; Rinaudo, M.; De Gennes, P. G. J. *Phys.* **1979**, 40, 701.
18. Plestil, J.; Ostanovich, Y. M.; Bezzabotonov, V. Y.; Hlavata, D.; Labsky, J. *Polymer* **1986**, 27, (6), 839-842.
19. Butler, J. A. V.; Conway, B. E. *Nature* **1953**, 172, (4369), 153-154.
20. Fujita, H.; Homma, T. *Journal of Colloid Science* **1954**, 9, (6), 591-601.
21. Tricot, M. *Macromolecules* **1984**, 17, (9), 1698-1704.
22. Nalwa, H. S., *Handbook of Polyelectrolytes and Their Applications*. American Scientific Publishers: July 2002.
23. Korolev, N.; Lyubartsev, A. P.; Nordenskiold, L. *Biophysical Journal* **1998**, 75, (6), 3041-3056.
24. Drukker, K.; Wu, G. S.; Schatz, G. C. *Journal of Chemical Physics* **2001**, 114, (1), 579-590.
25. Lin, S. C.; Lee, W. I.; Schurr, J. M. *Biopolymers* **1978**, 17, (4), 1041-1064.
26. Lee, W. I.; Schurr, J. M. *Journal of Polymer Science Part B-Polymer Physics* **1975**, 13, (5), 873-888.
27. Wilcoxon, J. P.; Schurr, J. M. *Journal of Chemical Physics* **1983**, 78, (6), 3354-3364.
28. Sedlak, M.; Konak, C.; Stepanek, P.; Jakes, J. *Polymer* **1987**, 28, (6), 873-880.
29. Schmitz, K. S.; Yu, J. W. *Macromolecules* **1988**, 21, (2), 484-493.
30. Amis, E. J.; Han, C. C. *Polymer* **1982**, 23, (10), 1403-1406.
31. Sedlak, M., *Physical Chemistry of Polyelectrolytes*. In CRC Press: New York, 2001.
32. Schmitz, K. S., *Macroions in Solution and Colloidal Suspension*. VCH Press:

New York, 1993.

33. Provencher, S. W. *Computer Physics Communications* **1982**, 27, (3), 229-242.
34. Provencher, S. W. *Computer Physics Communications* **1982**, 27, (3), 213-227.
35. Manning, G. S. *Journal of Chemical Physics* **1969**, 51, (8), 3249-&
36. Manning, G. S. *Journal of Chemical Physics* **1969**, 51, (3), 924-&
37. Oosawa, F. *Biopolymers* **1970**, 9, (6), 677-&
38. Schmitz, K. S.; Ramsay, D. J. *Biopolymers* **1985**, 24, 1247.
39. Schmitz, K. S.; Lu, M.; Gauntt, J. *Journal of Chemical Physics* **1983**, 78, (8), 5059-5066.
40. Lifson, S.; Katchalsky, A. *Journal of Polymer Science* **1954**, 13, (68), 43-55.
41. Degennes, P. G.; Pincus, P.; Velasco, R. M.; Brochard, F. *Journal De Physique* **1976**, 37, (12), 1461-1473.
42. Muthukumar, M. *Journal of Chemical Physics* **1996**, 105, (12), 5183-5199.
43. Muthukumar, M. *Journal of Chemical Physics* **1997**, 107, (7), 2619-2635.
44. Drifford, M.; Dalbiez, J. P. *Biopolymers* **1985**, 24, (8), 1501-1514.
45. Stigter, D. *Biopolymers* **1979**, 18, (12), 3125-3127.
46. Schmitz, K. S.; Lu, M.; Singh, N.; Ramsay, D. J. *Biopolymers* **1984**, 23, (9), 1637-1646.
47. Pusey, P. N.; Fijnaut, H. M.; Vrij, A. *Journal of Chemical Physics* **1982**, 77, (9), 4270-4281.
48. Benmouna, M.; Benoit, H.; Duval, M.; Akcasu, Z. *Macromolecules* **1987**, 20, (5), 1107-1112.
49. Brown, D. W.; Lowry, R. E. *Journal of Polymer Science Part a-Polymer Chemistry* **1979**, 17, (3), 759-768.
50. Baigl, D.; Seery, T. A. P.; Williams, C. E. *Macromolecules* **2002**, 35, (6), 2318-2326.

51. Nordmeier, E.; Dauwe, W. *Polymer Journal* **1992**, 24, (3), 229-238.
52. Nordmeier, E. *Polymer Journal* **1993**, 25, (1), 1-17.
53. Topp, A.; Belkoura, L.; Woermann, D. *Macromolecules* **1996**, 29, (16), 5392-5397.
54. Ermi, B. D.; Amis, E. J. *Macromolecules* **1998**, 31, (21), 7378-7384.
55. Sedlak, M. *J. Chem. Phys.* **1994**, 101, 10140.
56. Reed, W. F.; Ghosh, S.; Medjahdi, G.; Francois, J. *Macromolecules* **1991**, 24, (23), 6189-6198.
57. Michel, R. C.; Reed, W. F. *Biopolymers* **2000**, 53, (1), 19-39.
58. Sedlak, M. *Journal of Chemical Physics* **2002**, 116, (12), 5246-5255.
59. Smits, R. G.; Kuil, M. E.; Mandel, M. *Macromolecules* **1994**, 27, (20), 5599-5608.
60. Porsch, B.; Sundelof, L. O. *Macromolecules* **1995**, 28, (21), 7165-7170.
61. Sohn, D.; Russo, P. S.; Daila, A.; Poche, D. S.; McLaughlin, M. L. *Journal of Colloid and Interface Science* **1996**, 177, (1), 31-44.
62. Iddon, P. D.; Robinson, K. L.; Armes, S. P. *Polymer* **2004**, 45, (3), 759-768.
63. Borochoy, N.; Eisenberg, H. *Macromolecules* **1994**, 27, (6), 1440-1445.

APPENDIX A: PERMISSIONS

Letters of Permission:

For Figure 1.2

Dear Xiaowei,

You have our permission to use that image. However, I have attached possibly better ones, which are also unpublished. These are from a later work of David Heine and I, a summary of which was published in *Macromolecules*:

Structure of strongly charged polyelectrolyte solutions

J.P. Donley and D.R. Heine, *Macromolecules* 39, 8467 (2006).

So you can cite David and I for these if you use these unpublished images. They are from a larger and more realistic simulation. The first image, *asym.png*, is a 3-D snapshot of the whole simulation configuration at some late time in the simulation run (at equilibrium). The second is a zoomed-in portion (a spatial slice) of the configuration shown in the first image. Let us know if these are useful.

Regards,

James

For Figure 1.3:

Dear Xiaowei,

Please be advise permissions is granted to use the figure below in your forthcoming thesis at Louisiana State University and Agriculture and Mechanical College. Credit must appear on every copy using the material and must include the title; the author (s); and/or editor (s); Copyright (year and owner); and the statement "Reprinted with permission of John Wiley & Sons, Inc."

Please Note: No rights are granted to use content that appears in the work with credit to another source.

Sincerely,

Sheik Safdar| Permissions Coordinator| Global Rights - John Wiley & Sons, Inc.| 111 River St, MS 4-02

Hoboken, NJ 07030| Ph: 201-748-6512 | F: 201-748-6008| E: ssafdar@wiley.com

For Figure 1.4

2009/9/9

Copyright Clearance Center e-Licensi...

AMERICAN INSTITUTE OF PHYSICS LICENSE TERMS AND CONDITIONS

Sep 09, 2009

This is a License Agreement between Xiaowei Tong ("You") and American Institute of Physics ("American Institute of Physics") provided by Copyright Clearance Center ("CCC"). The license consists of your order details, the terms and conditions provided by American Institute of Physics, and the payment terms and conditions.

All payments must be made in full to CCC. For payment instructions, please see information listed at the bottom of this form.

License Number	2265020536899
License date	Sep 09, 2009
Licensed content publisher	American Institute of Physics
Licensed content publication	Journal of Chemical Physics
Licensed content title	Influence of ionic strength on the diffusion of polystyrene latex spheres, bovine serum albumin, and polynucleosomes@f[sup a]@f[sup]]
Licensed content author	Kenneth S. Schmitz, Mei Lu, Jennifer Gauntt
Licensed content date	Apr 15, 1983
Volume number	78
Issue number	8
Type of Use	Thesis/Dissertation
Requestor type	Student
Format	Electronic
Portion	Figure/Table
Number of figures/tables	3
Title of your thesis / dissertation	A Novel Synthesis and Characterization of Fluorescein Isothiocyanate Labeled Poly(styrenesulfonate sodium salt)
Expected completion date	Dec 2009
Estimated size (number of pages)	70
Total	0.00 USD

Terms and Conditions

American Institute of Physics -- Terms and Conditions: Permissions Uses

American Institute of Physics ("AIP") hereby grants to you the non-exclusive right and license to use and/or distribute the Material according to the use specified in your order, on a one-time basis, for the specified term, with a maximum distribution equal to the number that you have ordered. Any links or other content accompanying the Material are not the subject of this license.

1. You agree to include the following copyright and permission notice with the reproduction of the Material: "Reprinted with permission from [FULL CITATION]. Copyright

[PUBLICATION YEAR], American Institute of Physics." For an article, the copyright and permission notice must be printed on the first page of the article or book chapter. For photographs, covers, or tables, the copyright and permission notice may appear with the Material, in a footnote, or in the reference list.

2. If you have licensed reuse of a figure, photograph, cover, or table, it is your responsibility to ensure that the material is original to AIP and does not contain the copyright of another entity, and that the copyright notice of the figure, photograph, cover, or table does not indicate that it was reprinted by AIP, with permission, from another source. Under no circumstances does AIP, purport or intend to grant permission to reuse material to which it does not hold copyright.
3. You may not alter or modify the Material in any manner. You may translate the Material into another language only if you have licensed translation rights. You may not use the Material for promotional purposes. AIP reserves all rights not specifically granted herein.
4. The foregoing license shall not take effect unless and until AIP or its agent, Copyright Clearance Center, receives the Payment in accordance with Copyright Clearance Center Billing and Payment Terms and Conditions, which are incorporated herein by reference.
5. AIP or the Copyright Clearance Center may, within two business days of granting this license, revoke the license for any reason whatsoever, with a full refund payable to you. Should you violate the terms of this license at any time, AIP, American Institute of Physics, or Copyright Clearance Center may revoke the license with no refund to you. Notice of such revocation will be made using the contact information provided by you. Failure to receive such notice will not nullify the revocation.
6. AIP makes no representations or warranties with respect to the Material. You agree to indemnify and hold harmless AIP, American Institute of Physics, and their officers, directors, employees or agents from and against any and all claims arising out of your use of the Material other than as specifically authorized herein.
7. The permission granted herein is personal to you and is not transferable or assignable without the prior written permission of AIP. This license may not be amended except in a writing signed by the party to be charged.
8. If purchase orders, acknowledgments or check endorsements are issued on any forms containing terms and conditions which are inconsistent with these provisions, such inconsistent terms and conditions shall be of no force and effect. This document, including the CCC Billing and Payment Terms and Conditions, shall be the entire agreement between the parties relating to the subject matter hereof.

This Agreement shall be governed by and construed in accordance with the laws of the State of New York. Both parties hereby submit to the jurisdiction of the courts of New York County for purposes of resolving any disputes that may arise hereunder.

Gratis licenses (referencing \$0 in the Total field) are free. Please retain this printable license for your reference. No payment is required.

If you would like to pay for this license now, please remit this license along with your payment made payable to "COPYRIGHT CLEARANCE CENTER" otherwise you will be invoiced within 30 days of the license date. Payment should be in the form of a check or money order referencing your account number and this license number 2265020536899. If you would prefer to pay for this license by credit card, please go to <http://www.copyright.com/creditcard> to download our credit card payment authorization form.

For Figure 1.5, Figure 1.6, and Figure 1.7

AMERICAN INSTITUTE OF PHYSICS LICENSE TERMS AND CONDITIONS

Sep 20, 2009

This is a License Agreement between Xiaowei Tong ("You") and American Institute of Physics ("American Institute of Physics") provided by Copyright Clearance Center ("CCC"). The license consists of your order details, the terms and conditions provided by American Institute of Physics, and the payment terms and conditions.

All payments must be made in full to CCC. For payment instructions, please see information listed at the bottom of this form.

License Number	2270950108257
License date	Sep 16, 2009
Licensed content publisher	American Institute of Physics
Licensed content publication	Journal of Chemical Physics
Licensed content title	Dynamics of moderately concentrated salt-free polyelectrolyte solutions: Molecular weight dependence
Licensed content author	Marian Sedlak, Eric J. Amis
Licensed content date	Jan 1, 1992
Volume number	96
Issue number	1
Type of Use	Thesis/Dissertation
Requestor type	Student
Format	Electronic
Portion	Figure/Table
Number of figures/tables	2
Title of your thesis / dissertation	A Novel Synthesis and Characterization of Fluorescein Isothiocyanate Labeled Poly(styrenesulfonate sodium salt)
Expected completion date	Dec 2009
Estimated size (number of pages)	70
Total	0.00 USD

Terms and Conditions

American Institute of Physics -- Terms and Conditions: Permissions Uses

American Institute of Physics ("AIP") hereby grants to you the non-exclusive right and license to use and/or distribute the Material according to the use specified in your order, on a one-time basis, for the specified term, with a maximum distribution equal to the number that you have ordered. Any links or other content accompanying the Material are not the subject of this license.

1. You agree to include the following copyright and permission notice with the reproduction of the Material: "Reprinted with permission from [FULL CITATION]. Copyright [PUBLICATION YEAR], American Institute of Physics." For an article, the copyright and permission notice must be printed on the first page of the article or book chapter. For photographs, covers, or tables, the copyright and permission notice may appear with the

Material, in a footnote, or in the reference list.

2. If you have licensed reuse of a figure, photograph, cover, or table, it is your responsibility to ensure that the material is original to AIP and does not contain the copyright of another entity, and that the copyright notice of the figure, photograph, cover, or table does not indicate that it was reprinted by AIP, with permission, from another source. Under no circumstances does AIP, purport or intend to grant permission to reuse material to which it does not hold copyright.
3. You may not alter or modify the Material in any manner. You may translate the Material into another language only if you have licensed translation rights. You may not use the Material for promotional purposes. AIP reserves all rights not specifically granted herein.
4. The foregoing license shall not take effect unless and until AIP or its agent, Copyright Clearance Center, receives the Payment in accordance with Copyright Clearance Center Billing and Payment Terms and Conditions, which are incorporated herein by reference.
5. AIP or the Copyright Clearance Center may, within two business days of granting this license, revoke the license for any reason whatsoever, with a full refund payable to you. Should you violate the terms of this license at any time, AIP, American Institute of Physics, or Copyright Clearance Center may revoke the license with no refund to you. Notice of such revocation will be made using the contact information provided by you. Failure to receive such notice will not nullify the revocation.
6. AIP makes no representations or warranties with respect to the Material. You agree to indemnify and hold harmless AIP, American Institute of Physics, and their officers, directors, employees or agents from and against any and all claims arising out of your use of the Material other than as specifically authorized herein.
7. The permission granted herein is personal to you and is not transferable or assignable without the prior written permission of AIP. This license may not be amended except in a writing signed by the party to be charged.
8. If purchase orders, acknowledgments or check endorsements are issued on any forms containing terms and conditions which are inconsistent with these provisions, such inconsistent terms and conditions shall be of no force and effect. This document, including the CCC Billing and Payment Terms and Conditions, shall be the entire agreement between the parties relating to the subject matter hereof.

This Agreement shall be governed by and construed in accordance with the laws of the State of New York. Both parties hereby submit to the jurisdiction of the courts of New York County for purposes of resolving any disputes that may arise hereunder.

Gratis licenses (referencing \$0 in the Total field) are free. Please retain this printable license for your reference. No payment is required.

If you would like to pay for this license now, please remit this license along with your payment made payable to "COPYRIGHT CLEARANCE CENTER" otherwise you will be invoiced within 30 days of the license date. Payment should be in the form of a check or money order referencing your account number and this license number 2270950108257. If you would prefer to pay for this license by credit card, please go to <http://www.copyright.com/creditcard> to download our credit card payment authorization form.

**Make Payment To:
Copyright Clearance Center
Dept 001
P.O. Box 843006
Boston, MA 02284-3006**

For Figure 1.8, Figure 1.11, and Figure 1.12

Dear Xiaowei Tong,

With reference to your request (copy herewith) to reprint material on which Springer Science and Business Media controls the copyright, our permission is granted, free of charge, for the use indicated in your enquiry.

This permission

- allows you non-exclusive reproduction rights throughout the World.
- permission includes use in an electronic form, provided that content is
 - * password protected;
 - * at intranet;
- excludes use in any other electronic form. Should you have a specific project in mind, please reapply for permission.
- requires a full credit (Springer/Kluwer Academic Publishers book/journal title, volume, year of publication, page, chapter/article title, name(s) of author(s), figure number(s), original copyright notice) to the publication in which the material was originally published, by adding: with kind permission of Springer Science and Business Media.

The material can only be used for the purpose of defending your dissertation, and with a maximum of 40 extra copies in paper.

Permission free of charge on this occasion does not prejudice any rights we might have to charge for reproduction of our copyrighted material in the future.

Kind regards,
Estella Jap A Joe
Springer
Rights & Permissions

—

Van Godewijckstraat 30 | 3311 GX
P.O. Box 990 | 3300 AZ
Dordrecht | The Netherlands
fax +31 (0) 78 657 6377
estella.japajoe@springer.com

APPENDIX B: LIST OF ABBREVIATIONS AND SYMBOLS

BPT	Bromo- <i>p</i> -toluic acid
bpy	2,2'-bipyridine
DLS	Dynamic Light Scattering
FITC	Fluorescein isothiocyanate isomer I
FPR	Fluorescence Photobleaching Recovery
GPC/MALLS	Gel Permeation Chromatography/Multi Angle Laser Light Scattering
NaPSS	Poly(styrenesulfonate sodium salt)
NMR	Nuclear Magnetic Resonance
THF	Tetrahydrofuran
c_s	Concentration of salt in solutions
c_p	Concentration of polyelectrolytes in solutions
D	Self-diffusion coefficient
D_m	Mutual diffusion coefficient
D_s	Slow mode diffusion coefficient
D_f	Fast mode diffusion coefficient
e	Electron Charge
ε	Dielectric permittivity

F	Fluorescence intensity
F_0	Pre-bleach intensity
$F(0)$	Immediate post-bleach intensity
K	Spatial frequency
k	Bleaching depth
k_B	Boltzmann's constant
n	Refractive index
q	Scattering vector
T	Temperature
α	Ratio of the molar concentration of added counterions to the monomer concentration of the polyions
τ	Correlation time
Γ	Decay rate
λ	Wavelength
θ	Scattering angle

VITA

Xiaowei Tong was born in Hangzhou, Zhejiang, People's Republic of China, in 1983. She lived beside the beautiful West Lake until her graduation from Xuejun High School in 2002. She then attended Zhejiang University, Zhejiang, China, and obtained the Bachelor of Science degree in polymer materials and engineering. Following her graduation in 2006, Miss. Tong entered Academ Shen Zhiquan's group, Zhejiang University, as a research assistant in polymer synthesis.

In the Fall of 2007, Miss Tong entered chemistry department at Louisiana State University, and worked towards a master's degree in chemistry in December 2009.